Department of Applied Physics

Monte Carlo methodologies for neutron streaming in diffusion calculations

Application to directional diffusion coefficients and leakage models in XS generation

Eric Dorval

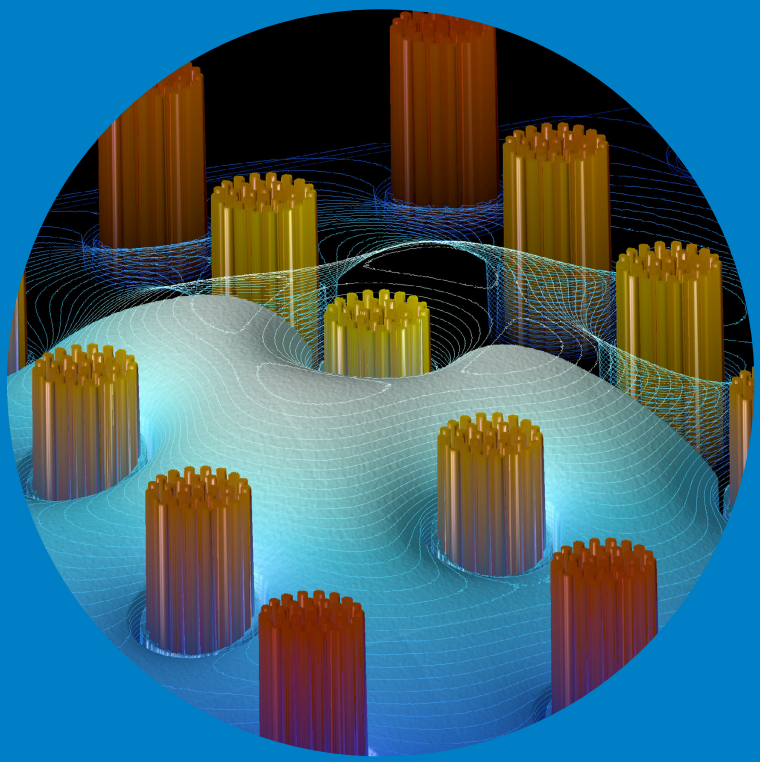

Aalto University

DOCTORAL DISSERTATIONS

Aalto University publication series
DOCTORAL DISSERTATIONS 60/2016

Monte Carlo methodologies for neutron streaming in diffusion calculations

Application to directional diffusion coefficients and leakage models in XS generation

Eric Dorval

A doctoral dissertation completed for the degree of Doctor of Science (Technology) to be defended, with the permission of the Aalto University School of Science, at a public examination held at the lecture hall K216 of the school on 18 May 2016 at 13.

Aalto University
School of Science
Department of Applied Physics
Antimatter and Nuclear Engineering

Supervising professor
Prof. Filip Tuomisto, Aalto University, Finland

Thesis advisor
Adj. Prof. Jaakko Leppänen, VTT Technical Research Centre of Finland Ltd

Preliminary examiners
Assoc. Prof. Wilfred van Rooijen, University of Fukui, Japan
Dr. Emil Fridman, Helmholtz-Zentrum Dresden-Rossendorf, Germany

Opponent
Dr. Eugene Shwageraus, University of Cambridge, United Kingdom

Aalto University publication series
DOCTORAL DISSERTATIONS 60/2016

ISBN 978-952-60-6735-3 (printed)
ISBN 978-952-60-6736-0 (pdf)
ISSN-L 1799-4934
ISSN 1799-4934 (printed)
ISSN 1799-4942 (pdf)
http://urn.fi/URN:ISBN:978-952-60-6736-0

Images: Eric Dorval

Unigrafia Oy
Helsinki 2016

Finland

441 697
Printed matter

Aalto University

Abstract

Aalto University, P.O. Box 11000, FI-00076 Aalto www.aalto.fi

Author
Eric Dorval

Name of the doctoral dissertation
Monte Carlo methodologies for neutron streaming in diffusion calculations - Application to directional diffusion coefficients and leakage models in XS generation

Publisher School of Science

Unit Department of Applied Physics

Series Aalto University publication series DOCTORAL DISSERTATIONS 60/2016

Field of research Engineering Physics

Manuscript submitted 19 January 2016 **Date of the defence** 18 May 2016

Permission to publish granted (date) 30 March 2016 **Language** English

☐ **Monograph** ☒ **Article dissertation** ☐ **Essay dissertation**

Abstract

Neutron transport calculations by Monte Carlo methods are finding increased application in nuclear reactor simulations. In particular, a versatile approach entails the use of a 2-step procedure, with Monte Carlo as a few-group cross section data generator at lattice level, followed by deterministic multi-group diffusion calculations at core level.

In this thesis, the Serpent 2 Monte Carlo reactor physics burnup calculation code is used in order to test a set of diffusion coefficient models, as well as neutron leakage methodologies at assembly level. The tests include novel anisotropic diffusion coefficient and heterogeneous leakage models developed and implemented by the author.

The analyses are mainly focused on a sodium-cooled fast reactor system, for which few-group cross section data was generated by stochastic methods with Serpent 2. The quality of the full-core diffusion results is evaluated by contrasting system eigenvalues and power distributions against detailed, full-core reference solutions also supplied by the Serpent 2 code and the same nuclear data library.

Whereas the new anisotropic diffusion coefficient formalism exhibits improved performance in the fast reactor system studied, there are restrictions to its applicability in other reactor designs. The newly proposed leakage model has a similar performance to that one of albedo iterations, and provides valuable information about the space-energy coupling of the scalar neutron flux at lattice level. This hitherto unavailable information does not entail a significant computational cost.

In sodium-cooled fast reactor calculations, the quality of diffusion theory results can be improved by either using directional diffusion coefficients and a fine energy mesh, or via leakage-corrected discontinuity factors. These factors can be calculated using net neutron currents supplied by heterogeneous leakage models. Preliminary results from this research also suggest that the studies maybe extended to graphite-moderated, gas-cooled reactors.

Keywords Monte Carlo, Serpent, directional diffusion coefficient, TRIZ, TRIVAC, neutron leakage, layer expansion, albedo, B1, discontinuity factor, SFR

ISBN (printed) 978-952-60-6735-3 **ISBN (pdf)** 978-952-60-6736-0

ISSN-L 1799-4934 **ISSN (printed)** 1799-4934 **ISSN (pdf)** 1799-4942

Location of publisher Helsinki **Location of printing** Helsinki **Year** 2016

Pages 155 **urn** http://urn.fi/URN:ISBN:978-952-60-6736-0

Preface

The work presented in this thesis was conducted at the Fission and Radiation Physics Group at Aalto University School of Science, Department of Applied Physics.

I would like to express my gratitude towards the two supervising professors who led the group during my studies: Rainer Salomaa and Filip Tuomisto. In particular, I would like to thank Professor Salomaa, for his trust allowed me to take on studies in Finland. My sincerest recognition also goes to the advisor of this thesis, Dr. Jaakko Leppänen, for his eagerness to contribute towards the improvement of my work. Dr. Leppänen's development of the Serpent Monte Carlo code founded the basis for many a thesis, and this work is not an exception.

The pre-examiners of this thesis are acknowledged for their valuable, constructive comments and observations. I am grateful for their contributions towards the clarity of this work. As for my colleagues at Aalto, I would like to thank them for the nice working atmosphere. In particular, I am indebted to Dr. Pertti Aarnio and to Risto Vanhanen for commenting on my manuscripts.

The financial resources supplied by the YTERA Doctoral Programme for Nuclear Engineering and Radiochemistry were indispensable for the fulfillment of this research. Special recognition goes to Dr. Jarmo Ala-Heikkilä for his impeccable coordination of the programme.

In times of supercomputing, the results of this thesis were procured by making extensive use of the resources provided by the Aalto Science-IT project, in the form of the Triton cluster and its associated support, and by the CSC IT Centre for Science, Ltd., via the Taito supercluster and its support team.

Formality rules relegate acknowledgements towards family members and friends, from both near and afar, to the very end of this preface. This ordering, however, does not do justice to their permanent encouragement and

enthusiasm. This work is the culmination of a long journey which began with my parents' love, honesty, dedication and knowledge. I thank them for raising free-minded children.

I will be forever obliged to Instituto Balseiro in Argentina for the excellent education I received during my engineering and masters studies. Also, I would like to sincerely give thanks to a few people who played a decisive role in my career through their superlative professional standards and their human integrity: María Arribére, Abraham Kestelman and Oscar Zamonsky.

I apologize for not finding the right words to thank my wife Salla for her crucial support during all this time. You give meaning to so many things.

Espoo, March 30, 2016,

Eric Dorval

Contents

List of Publications

This thesis consists of an overview and of the following publications which are referred to in the text by their Roman numerals.

I E. Dorval. A New Method for the Calculation of Diffusion Coefficients with Monte Carlo. In *Proceedings of the Joint International Conference on Supercomputing in Nuclear Applications and Monte Carlo 2013 (SNA + MC 2013)*, Paris, 02204, http://dx.doi.org/10.1051/snamc/201402204, 2014.

II E. Dorval and J. Leppänen. Monte Carlo current-based diffusion coefficients: Application to few-group constants generation in Serpent. *Annals of Nuclear Energy*, **78**, pp. 104–116, http://dx.doi.org/10.1016/j.anucene.2014.12.011, 2015.

III E. Dorval. Directional diffusion coefficients and leakage-corrected discontinuity factors: Implementation in Serpent and tests. *Annals of Nuclear Energy*, **87**, pp. 101–112, http://dx.doi.org/10.1016/j.anucene.2015.08.019, 2016.

IV E. Dorval. A Comparison of Monte Carlo methods for neutron leakage at assembly level. *Annals of Nuclear Energy*, **87**, pp. 591–600, http://dx.doi.org/10.1016/j.anucene.2015.10.014, 2016.

V E. Dorval. A comparative study of leakage and diffusion coefficient models for few-group cross section generation with the Monte Carlo method. *Annals of Nuclear Energy*, **90**, pp. 353–363, http://dx.doi.org/10.1016/j.anucene.2015.12.021, 2016.

Author's Contribution

Publication I: "A New Method for the Calculation of Diffusion Coefficients with Monte Carlo"

The author was the sole contributor to this work.

Publication II: "Monte Carlo current-based diffusion coefficients: Application to few-group constants generation in Serpent"

The author implemented the anisotropic diffusion coefficient calculation routine in the Serpent code and generated the reference and cross section data. The author wrote the diffusion code TRIZ, performed the diffusion calculations and analyzed the results. The author wrote this publication.

Publication III: "Directional diffusion coefficients and leakage-corrected discontinuity factors: Implementation in Serpent and tests"

The author was the sole contributor to this work.

Publication IV: "A Comparison of Monte Carlo methods for neutron leakage at assembly level"

The author was the sole contributor to this work.

Publication V: "A comparative study of leakage and diffusion coefficient models for few-group cross section generation with the Monte Carlo method"

The author was the sole contributor to this work.

1. Introduction

1.1 Background

The world's need for energy is expected to keep its growing trend in the foreseeable future, mainly driven by developing countries. Large-scale deforestation and the burning of fossil fuel in order to meet the world's energy demand has lead to a systematic increase in the concentrations of greenhouse gases in the atmosphere [1]. These gases, primarily in the form of carbon dioxide (CO_2), are precipitating climate change.

Nuclear fusion is a promising technology for the production of abundant and sustainable energy [2]. Its commercial deployment, however, is not envisaged in the near future. Based on current operating technology, available resources and prospects for innovation, nuclear fission reactors can provide CO_2-free electricity in large quantities.

The Gen-IV International Forum [3] has identified Sodium-cooled Fast Reactor (SFR) designs [4] as auspicious suitors to fulfill the goals of safety, sustainability, reliability, proliferation resistance and economic competitiveness. In order to improve the performance features of previous designs, taking lessons learned into account, the use of sophisticated computational tools, or "codes", is indispensable.

A nuclear fission reactor is a complex system that involves multiple physical phenomena, which extend over wide ranges in the time, space, and energy domains. Over the years, numerous dedicated methodologies and suites of computer codes, such as `ERANOS` [5] and `FAST` [6], have been developed towards the study of fast reactor systems.

In the field of neutronics, the so-called stochastic, or Monte Carlo (MC) techniques are finding increased application. Although full-core calculations with these techniques are feasible, they can be computationally very

demanding. A more efficient approach exploits a so-called 2-step calculation procedure, via the use of a Monte Carlo few-group cross section (XS) constant generation code at lattice level, and a deterministic neutron diffusion solver applied to full-core reactor calculations with piecewise homogenized zones. The works by Fridman et al. [7] and by Nikitin et al. [8] provide examples of the 2-step approach applied to fast reactor systems.

The computation of neutron diffusion coefficients in general, and of directional diffusion coefficients in particular, remains an open problem in the context of Monte Carlo few-group XS generation. In addition to diffusion coefficients, the treatment of neutron leakage at assembly level can have an effect on the quality of the final diffusion results.

Traditionally, most diffusion coefficient models were contrasted by direct comparison of their results. Nowadays, the availability of more efficient Monte Carlo codes and modern, large parallel computing facilities allows the procurement of detailed solutions to the problem of neutron transport in complete, three-dimensional (3-D) reactor systems. These solutions constitute the best references for the performance appraisal of diffusion coefficient and neutron leakage models when applied to their ultimate goal: the calculation of full-core problems by diffusion solvers.

1.2 Objectives and scope

The aim of this thesis is to characterize the performance of and to propose improvements to a variety of methods adopted by some few-group XS generation codes, with a view towards full-core calculations by neutron diffusion theory. In particular, the studies are related to diffusion coefficients and means of characterizing neutron leakage at assembly level by Monte Carlo methods. The objective of this thesis is twofold, and can be cast into the form of two research questions (RQs):

RQ1: *How satisfactory is the performance and what are the limitations of neutron diffusion coefficients generated by preexisting deterministic and novel Monte-Carlo-specific methods when applied to 3-D, full-core diffusion calculations, with special emphasis on sodium-cooled fast reactors?*

RQ2: *In the context of Monte Carlo few-group constants generation, what is the effect of different strategies to cater for neutron leakage at assembly level on the quality of single assembly pin powers, full-core diffusion eigenvalues and power distributions?*

These research questions are interconnected. As will be exposed in the following chapter, the streaming of neutrons in the diffusion equation is captured by a term involving the diffusion coefficient. Also, some MC methodologies resort to a form of buckling-based leakage for the computation of diffusion coefficients, or even explicitly require a net leakage of neutrons from the system.

This thesis excludes thermal-hydraulic (T-H) aspects and time-dependent studies, as well as the isotopic changes that occur as a result of material irradiation by neutrons and subsequent radioactive decay. This work does not address the propagation of uncertainties associated with basic nuclear data nor physics models.

Uncertainties in the diffusion results linked to the statistical nature of the few-group XS data generated by Monte Carlo techniques are not considered here. These uncertainties are, however, estimated in the corresponding publications. The criterion for the selection of the results to be included and compared in this thesis is that those values are significantly different in a statistical sense. When necessary, clarifications will be made in cases where the results are comparable within their statistical uncertainties.

1.3 Research process and dissertation structure

The entirety of this thesis relies on results procured via computer simulations. Most of the calculations and proposed methodologies were implemented and tested in the Monte Carlo code `Serpent` [9], using basic nuclear data from the JEFF-3.1 library [10]. Diffusion calculations were conducted with the in-house code `TRIZ` [11], developed by the author, and with the code `TRIVAC` [12].

This thesis is supported by selected findings from Publications I–V. Each one of the two research questions from Section 1.2 is addressed by a dedicated chapter, and not by a single article. This arrangement obeys the incremental way in which the research was conducted in practice. In order to assist the understanding of how RQs are addressed, the article relations among themselves and with the research questions are illustrated in Fig. 1.1.

The rest of this thesis is structured as follows: Chapter 2 formalizes the definition of the research problem by providing a more comprehensive overview of the theoretical and methodological aspects associated with the research questions. Chapters 3 and 4 are devoted to RQ1 and RQ2, respectively, through a presentation of results and by discussing their rele-

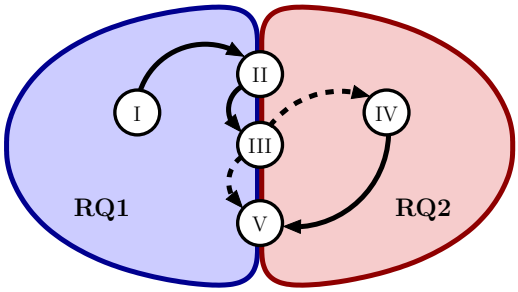

Figure 1.1. The interplay among articles and research questions in this thesis. Publications are identified by Roman numerals. A full arrow line indicates that a publication incorporates strong developmental or investigation needs raised by its predecessor. A dashed arrow line indicates a non-essential study or developmental need from its predecessor.

vance. Finally, Chapter 5 summarizes the main conclusions, limitations, and prospects for future work.

2. Theoretical foundation and methods

In this chapter, the main theoretical aspects of the numerical modeling of nuclear reactor neutronics are outlined, with special emphasis on the methods used in Publications I–V. The application of the methods presented herein to the research problem addressed in this thesis is left to Chapters 3 and 4. Many of the equations found in the literature have undergone changes in notation so that a unified nomenclature is followed throughout the thesis.

2.1 Neutron transport: the Boltzmann equation

The behavior of neutrons in a given volume V, when neutron-to-neutron interactions are neglected, is described by the *linear Boltzmann transport equation*. In its general form, this time-dependent equation is coupled to the *delayed neutron precursors equations*, which describe the temporal evolution of neutrons born upon decay of a special set of fission products, as well as to the *burnup equations*, which govern the nuclide inventories as a result of neutron irradiation. Moreover, the neutron transport equation is coupled to the *T-H equations*.

In this thesis, it is assumed that the nuclide inventory and temperature distributions in the system are known and fixed. The attention will be focused on the so-called *steady-state neutron transport equation* [13], in absence of external neutron sources:

$$\begin{aligned} \hat{\Omega}\cdot\nabla\psi\left(\vec{r},\hat{\Omega},E\right)+\Sigma_t\left(\vec{r},E\right)\,\psi\left(\vec{r},\hat{\Omega},E\right) \\ =\int_0^\infty\int_{4\pi}\Sigma_s\left(\vec{r},\hat{\Omega}\cdot\hat{\Omega}',E'\to E\right)\,\psi\left(\vec{r},\hat{\Omega}',E'\right)d\hat{\Omega}'\,dE' \\ +\frac{\chi(\vec{r},E)}{4\pi\,k}\int_0^\infty\int_{4\pi}\nu\Sigma_f(\vec{r},E')\,\psi\left(\vec{r},\hat{\Omega}',E'\right)d\hat{\Omega}'\,dE', \\ \vec{r}\in V,\,\hat{\Omega}\in 4\pi,\,0<E<\infty, \\ \psi\left(\vec{r},\hat{\Omega},E\right)=0,\,\vec{r}\in\partial V,\,\hat{\Omega}\cdot\hat{n}<0. \end{aligned} \tag{2.1}$$

The transport equation can be cast in a number of different ways. Eq. (2.1) uses the integro-differential form. The quantities involved are:

$\vec{r}$: position vector.

$\hat{\Omega}$: direction vector.

E : kinetic energy.

ψ : angular neutron flux.

Σ_t : total macroscopic cross section.

Σ_s : scattering macroscopic cross section.

$\nu\Sigma_f$: fission neutron production macroscopic cross section.

χ : fission spectrum.

k : effective multiplication factor, or criticality eigenvalue.

Another quantity of importance is the scalar neutron flux:

$$\phi\left(\vec{r}, E\right) = \int_{4\pi} \psi\left(\vec{r}, \hat{\Omega}, E\right) d\hat{\Omega}\,. \tag{2.2}$$

Specialized textbooks [13, 14] provide detailed descriptions of the derivation and physical interpretation of every term in Eq. (2.1). By omitting the temporal dependence, phenomena that take place at two substantially different time scales are neglected. In the shortest of these scales (of the order of seconds), the effect of delayed neutrons is not taken into account, whereas in a time scale that spans from hours to years, the isotopic changes that take place as a result of neutron-induced fission, activation, and subsequent decay are not considered. The latter changes, in turn, have an effect on the macroscopic cross sections of Eq. (2.1). Moreover, the thermal-hydraulic feedback commonly encountered during reactor transients is not considered, either

A nuclear reactor is a large heterogeneous system comprising a vast number of components, with typical length scales ranging from less than a millimeter to several tens of centimeters, which at the core level can result in systems of a few meters in the radial and axial directions. In practical applications, the energy variable E ranges from 10^{-11} MeV to around 10 MeV. As for the XS data, it can also experience several orders of magnitude variations along its energy domain. Moreover, the presence of resonances implies rapid variations within narrow energy ranges, as depicted in Fig. 2.1.

During a normal irradiation cycle, hundreds of different nuclides (with associated cross section sets) are present in a nuclear reactor core. In view of

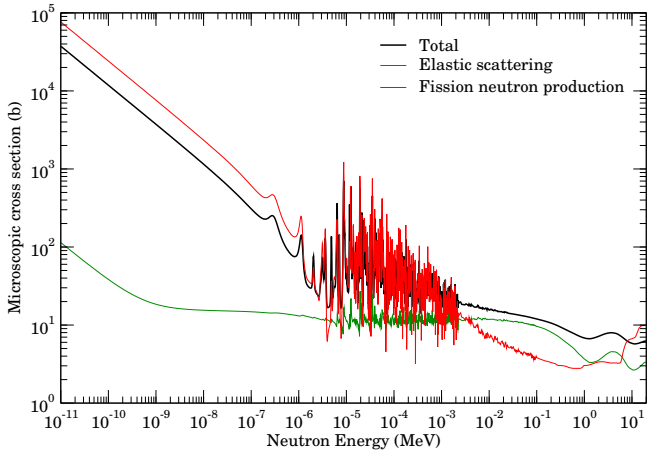

Figure 2.1. Microscopic reaction cross sections for incident neutrons on ^{235}U at 1173 K. Based on data from the JEFF-3.1 nuclear data library [10].

this, the direct solution of Eq. (2.1) lies beyond the capabilities of any analytical method. It is imperative to resort to numerical techniques. These can be classified into two categories: deterministic and stochastic. In what follows, these categories will be described. Prior to the introduction of stochastic methods, the 2-step calculation approach concept will be presented.

2.2 Deterministic techniques

These methods give solutions to discretized forms of Eq. (2.1). Whilst different methods entail particular discretization schemes and approximations for the treatment of the spatial and angular variables, in all cases the continuous energy domain is segmented into a number of energy bins or *groups*. This is known as the *multi-group* approximation [15].

Among the deterministic numerical methods developed for the solution of the neutron transport equation, a few are mentioned here, followed by computer codes where they are implemented:

- Spherical harmonics (SH or P_N): `EVENT` [16], `MARC` [17].
- Collision probabilities (CP): `WIMS-D` [18], `CONDOR` [19].
- Discrete ordinates method (S_N): `NEWT` [20], `XSDRNPM` [21].
- Method of characteristics (MoC): `CASMO-4` [22], `DRAGON` [23], `APOLLO2` [24], `HELIOS-2` [25].

With the exception of some particular forms of the spherical harmonics me-

thod, a thorough description of the deterministic numerical methods falls beyond the scope of this thesis. Although some of the aforementioned methods still are the subject of ongoing research, their foundations are described, for instance, in the review article by Sanchez and McCormick [26], as well as in the work by Lewis and Miller [15].

2.2.1 The P_1 approximation

In the P_N method, the angular dependence of the neutron flux is expanded in a spherical harmonics basis. In the P_N approximation, the infinite series used for the expansion of the flux is truncated at level N, thus resulting in $(N+1)$ terms. In particular, when $N = 1$ is set, the P_1 equations are obtained. Based on the expressions by Roy [27], and further making the fission term explicit, the time-independent P_1 equations without external sources in multi-group form are expressed as:

$$\nabla \cdot \vec{J}^g(\vec{r}) + \Sigma_t^g(\vec{r})\,\phi^g(\vec{r}) = \sum_{g'=1}^{G} \Sigma_{s,0}^{g \leftarrow g'}(\vec{r})\,\phi^{g'}(\vec{r}) + \frac{\chi^g}{k} \sum_{g'=1}^{G} \nu\Sigma_f^{g'}(\vec{r})\,\phi^{g'}(\vec{r})\,,$$

$$\frac{1}{3}\nabla\phi^g(\vec{r}) + \Sigma_t^g(\vec{r})\,\vec{J}^g(\vec{r}) = \sum_{g'=1}^{G} \Sigma_{s,1}^{g \leftarrow g'}(\vec{r})\,\vec{J}^{g'}(\vec{r})\,. \tag{2.3}$$

The first one of the P_1 Eqs. (2.3) is scalar, and in fact denotes a set of G multi-group equations, each one denoted by its group index g. The second of the P_1 equations is three dimensional, since $\vec{J}$ is the neutron current density vector. The scattering cross section was expanded in Legendre polynomials, thus $\Sigma_{s,0}$ and $\Sigma_{s,1}$ denote the zeroth and first order terms of this expansion, respectively.

2.2.2 The diffusion approximation

Three assumptions are needed in order to derive the diffusion equations from the P_1 equations:

The external source is isotropic: thus far, cases without external sources have been considered only. As for the fission source, it is isotropic.

Negligible temporal variation of the neutron current: since the time-independent P_1 equations are dealt with here, this assumption has no effect. In time-dependent kinetics problems, however, this simplification could be inadequate (and difficult to verify).

In- and out-scattering neutron source anisotropy: in multi-group form,

this approximation is expressed by:

$$\sum_{g'=1}^{G} \Sigma_{s,1}^{g \leftarrow g'}(\vec{r})\, \vec{J}^{g'}(\vec{r}) \simeq \sum_{g'=1}^{G} \Sigma_{s,1}^{g' \leftarrow g}(\vec{r})\, \vec{J}^{g}(\vec{r})\,. \tag{2.4}$$

Stamm'ler and Abbate [28] highlight that this approximation holds in presence of weak absorption only. Substitution of Eq. (2.4) into the second of the P_1 Eqs. (2.3) allows to switch the summation that extends over the incoming energies towards the outgoing energies:

$$\frac{1}{3}\nabla\phi^{g}(\vec{r}) + \Sigma_{t}^{g}(\vec{r})\, \vec{J}^{g}(\vec{r}) = \sum_{g'=1}^{G} \Sigma_{s,1}^{g' \leftarrow g}(\vec{r})\, \vec{J}^{g}(\vec{r}) \;= \Sigma_{s,1}^{g}(\vec{r})\, \vec{J}^{g}(\vec{r})\,. \tag{2.5}$$

Rearranging Eq. (2.5):

$$\vec{J}^{g}(\vec{r}) = -\frac{1}{3\left(\Sigma_{t}^{g}(\vec{r}) - \Sigma_{s,1}^{g}(\vec{r})\right)}\, \nabla\phi^{g}(\vec{r})\,, \tag{2.6}$$

one arrives at an expression that relates the neutron current with the gradient of the neutron flux. This is known as *Fick's law*, and is commonly expressed in terms of the *diffusion coefficient* D:

$$\vec{J}^{g}(\vec{r}) = -D^{g}(\vec{r})\, \nabla\phi^{g}(\vec{r})\,. \tag{2.7}$$

The diffusion coefficient is related to the *transport cross section*, Σ_{tr}, by:

$$D^{g}(\vec{r}) = \frac{1}{3\,\Sigma_{tr}^{g}(\vec{r})}\,. \tag{2.8}$$

In turn, the transport cross section is derived naturally from Eq. (2.6), and is expressed in terms of the total XS, the mean scattering cosine in the laboratory system, and the scattering cross section[1]:

$$\Sigma_{tr}^{g}(\vec{r}) = \Sigma_{t}^{g}(\vec{r}) - \overline{\mu_0^g}\, \Sigma_{s}^{g}(\vec{r})\,. \tag{2.9}$$

Hébert [30] remarks that Fick's law is a heuristic relation which, in a more general form, is expressed in terms of a 3×3 diagonal tensor $\mathbb{D}$, containing *directional diffusion coefficients*, such that:

$$\vec{J}^{g}(\vec{r}) = -\mathbb{D}^{g}(\vec{r})\, \nabla\phi^{g}(\vec{r})\,. \tag{2.10}$$

Fick's law is acceptable at the global[2] scale of a complete reactor, but breaks down at the level of heterogeneous lattice calculations. As will be seen in Section 2.3, homogenization techniques are used in order to decompose a full heterogeneous reactor system into a set of piecewise homogeneous regions.

[1] In order to arrive at Eq. (2.9), the identity $\Sigma_{s,1}^{g} = \overline{\mu_0^g}\, \Sigma_{s,0}^{g}$ was used [29].
[2] Either homogeneous or piecewise homogeneous.

By introducing Fick's law into the first of the P_1 Eqs. (2.3), the multi-group diffusion equations:

$$-\nabla\cdot D^g(\vec{r})\,\nabla\phi^g(\vec{r})+\Sigma_r^g(\vec{r})\,\phi^g(\vec{r})=\sum_{g'\neq g}\Sigma_{s,0}^{g\leftarrow g'}(\vec{r})\,\phi^{g'}(\vec{r})+\frac{\chi^g}{k}\sum_{g'=1}^{G}\nu\Sigma_f^{g'}(\vec{r})\,\phi^{g'}(\vec{r}) \tag{2.11}$$

are obtained. Self-scattering elements are excluded from the scattering source. This is compensated for by replacing the total XS with the *removal* cross section:

$$\Sigma_r^g=\Sigma_t^g-\Sigma_{s,0}^{g\leftarrow g}\,. \tag{2.12}$$

2.3 The 2-step calculation approach

Even after simplifications, the solution of detailed 3-D reactor systems using deterministic methods is a formidable task from the point of view of computational requirements. A low order transport method such as diffusion is only valid at the complete –homogenized– reactor level.

Other low order methods which are less restrictive, such as P_1 or simplified P_3 (also called SP_3) [31] are not much more than improved diffusion, and cannot tackle the challenge of accurately modeling a detailed –heterogeneous– reactor system, either. A work by Kotiluoto [32] stresses that the SP_3 approximation applied to heterogeneous transport is not always satisfactory. Conversely, Duerigen et al. [33] applied the SP_3 approximation to piecewise homogeneous regions, and observed good agreement with transport results.

The underlying idea of the 2-step methodology is to partition a large heterogeneous system into smaller sub-systems, or cells, in which some form of the neutron transport equation is solved. This solution is then used in order to *homogenize* such cell, so that as a result of this process the homogenized system furnishes the same reaction rates as the geometrically detailed system would. This is known as the first step, or assembly calculation, or lattice calculation, usually restricted to two-dimensional (2-D) geometry. Homogenized cross sections are generated assuming an infinite lattice of identical elements. This is attained in practice by applying reflective or periodic boundary conditions, with the exception of reflectors [34] and other non-multiplicative regions.

In the second step, a lower order form of the transport operator is solved at core level. Generally, this task is accomplished by diffusion theory. At this level, every heterogeneous cell has been replaced by a set of homogeneous, constant properties (supplied in the form of a homogenized XS set), in an

attempt to reproduce assembly-wise reaction rates as accurately as possible, so that the criticality eigenvalue of Eq. (2.1) is preserved in the original heterogeneous and in the homogeneous systems, at a much lower computational cost.

Prinja and Larsen [13] allege that homogenization is difficult to justify theoretically, and that there is ongoing debate about the proper manner in which homogenization should be performed. The use of flux-and-volume-weighting techniques is standard practice in the calculation of homogenized reaction cross sections in a zone denoted by i:

$$\Sigma_{\alpha,i}^{g,hom} = \frac{\sum\limits_{h\in g}\sum\limits_{j\in i}\Sigma_{\alpha,j}^{h}\,\phi_{j}^{h}\,V_{j}}{\sum\limits_{h\in g}\sum\limits_{j\in i}\phi_{j}^{h}\,V_{j}}\,, \tag{2.13}$$

where α identifies the type of reaction in a certain cell denoted by j, and h identifies a micro-energy index that lies within a few-group index g. In the infinite-medium limit, reaction rates in the heterogeneous and in the homogeneous systems are preserved. As for homogenized diffusion coefficients, Cho [35] discusses some of the difficulties that emerge from their computation. The root cause of the problem is that diffusion coefficients do not arise from a mere preservation of reaction rates.

Since the early days of lattice solvers based on the collision probability method, extensive work [36–43] has been conducted in order to find more accurate expressions to compute homogenized diffusion coefficients. Many of these works were targeted at anisotropic neutron diffusion in fast reactor systems.

In recent times, Williams [44] applied finite Fourier transform techniques to the calculation of anisotropic diffusion coefficients in one-dimensional (1-D) domains. Pounders and Rahnema [45] tested the performance of various diffusion closures for the improvement of accuracy between diffusion theory and transport solutions for 1-D problems. In spite of the vast number of studies conducted on diffusion coefficients, Prinja and Larsen [13] remark that:

> "the optimal definition of homogenized diffusion coefficients remains an unresolved problem."

The comparison of diffusion solutions against transport theory is an amenity that was not readily available in the early days.

2.3.1 Equivalence theory

The effect on core calculations of the seemingly arbitrary diffusion coefficient definitions is mitigated in the context of Equivalence Theory. Koebke [46] postulates that the errors introduced during the assembly homogenization process can be overcome by providing the diffusion equation with additional degrees of freedom, so that the average reaction rates, fluxes and neutron currents per homogenized region are preserved with regards to the original heterogeneous problem. In order to accomplish this, he relaxes the constraint of flux continuity at assembly boundaries through the introduction of *heterogeneity factors*.

Smith [47, 48] also recognizes the importance of allowing the fluxes to be discontinuous, and proposes an alternative scheme which avoids the iterative techniques devised by Koebke. By treating every homogenized assembly as a local problem, with net currents supplied by a global transport solution –assuming that it is available–, he shows that the continuity of flux at assembly boundaries is responsible for the homogenized currents to be different from the transport currents. In an attempt to preserve the reaction rates per assembly, as well as the global transport currents in the local diffusion solutions, the modification proposed is based on the concept of flux *discontinuity factors* (DFs), applied at assembly boundaries.

For a given face denoted by u, the discontinuity factor for group g is noted as f_g^u, and is defined as the ratio between the face-averaged heterogeneous scalar flux (obtained by transport methods) and the face-averaged scalar flux resulting from the application of diffusion theory with homogeneous XS data and identical boundary conditions:

$$f_g^u \equiv \frac{\phi_g^{u,het}}{\phi_g^{u,hom}} \,. \tag{2.14}$$

Although the works by Koebke and by Smith were mainly targeted at high order nodal methods and steady-state problems, Sutton and Aviles [49], for example, make the applicability of equivalence theory to kinetics calculations explicit. Furthermore, discontinuity factors can also be applied to finite-difference-based solvers, as outlined by DeLorey [50].

2.3.2 Spatial discretization of the diffusion equations

The multi-group diffusion Eqs. (2.11) are continuous in the spatial variable. As a result of homogenization, XS data is assumed to be constant over the volume of every lattice element. In order to solve for the equations numeri-

cally, some form of discretization is needed.

The first discretization schemes resorted to finite differences, where the derivative term in Eq. (2.11) was approximated by a varying number of discrete points [51]. The discretized equations were then solved in the form of linear systems with special iteration strategies for the determination of the system eigenvalue and multi-group fluxes [52]. Some examples of finite-difference-based diffusion codes are: `CITATION` [53] and `DIF3D` [54].

The discretization of differential equations brings about some extent of error. Methods have been developed in order to palliate this [55], and were applied, for example, to the calculation of "extrapolated" solutions of benchmark problems [56, 57]. It is interesting to notice that the corrections proposed are closely related to the very early studies by Richardson [58] and by Richardson and Gaunt [59], before the invention of electronic computers.

Modern diffusion solvers resort to the so-called *nodal methods*, which take advantage of scalar neutron flux expansions, so that the number of unknowns to be solved for is kept low, yet the solution is highly accurate. An excellent review of nodal methods may be found in the work by Lawrence [60]. The schemes reported therein resort to the decomposition of the full problem into 1-D transverse-integrated equations.

Whereas the transverse integration technique has shown a high degree of success in Cartesian geometry, its application to hexagonal problems results in singular terms, which need to be dealt with carefully. For this reason, more recent alternative techniques have been developed for the solution of the nodal diffusion equations in hexagonal geometry, such as conformal mapping [61, 62], Analytical Function Expansion Nodal [63], and Higher Order Polynomial Expansion Nodal [64]. A few examples of nodal diffusion codes are: `PARCS` [65], `ARES` [66], and `DYN3D` [67].

In contrast to Cartesian geometry, it is not possible to resort to mesh refinement in hexagonal problems, unless the domain is decomposed into triangles. In the hypothetical case where the quality of the nodal solution is suspected to be compromised as a result of the inability of a low order flux expansion to capture sharp flux variations within an assembly, then it might be a better choice to sacrifice computational efficiency by resorting to finite-difference codes, instead.

2.4 Stochastic techniques

The use of stochastic techniques is commonly known as the Monte Carlo method [68, 69]. This powerful method is based on the simulation of stochastic processes using computer-generated pseudo-random numbers and by sampling different events with probabilities given by the laws that govern such processes. The Monte Carlo method can be applied to mathematical, physical and engineering problems, amongst several others.

The application of Monte Carlo techniques to neutron transport is extensively presented in specialized references [70, 71, and references therein]. The main advantages of the MC method applied to reactor calculations are the possibility of modeling complex systems with virtually no geometrical approximations; the detailed treatment of the neutron interaction models; and parallelization. Some examples of general purpose Monte Carlo particle transport codes are: `MCNP` [71], `TRIPOLI` [72], `VIM` [73], and `MCBEND` [74].

Any Monte Carlo result –or tally– is subject to some extent of statistical uncertainty due to the finite size of the number of samples, or neutron histories simulated. According to the Central Limit Theorem, the estimated mean of a number of identically distributed, *independent* random variables will appear to be normally distributed, with a standard deviation:

$$\sigma_m = \sigma/\sqrt{N}, \tag{2.15}$$

as the number of samples, N, approaches infinity. The standard deviation σ is approximated [75] by the square root of the observed sample variance, s^2.

Eq. (2.15) implies that the statistical uncertainty of Monte Carlo results can be reduced by the computation of more neutron histories, thus increasing the value of N. However, the $1/\sqrt{N}$ dependence with the number of histories entails an extra computational burden that renders the MC approach impractical for several everyday neutron transport calculations. Also, the method can be prone to bias [76] and false convergence, which need to be carefully assessed. In addition, Martin [77] underlines an excessive demand on computer memory, slow convergence of the fission source, and an underestimation[3] of the true variance. Mervin and others [78] propose remedies to mitigate this.

In spite of these limitations, Monte Carlo methods are finding increased application in the context of few-group cross section generation, thanks to their high geometrical fidelity and continuous-energy neutron interaction

[3] This is due to the fact that neutron histories are correlated, in contrast with the assumptions of the Central Limit Theorem.

models. Examples of codes that can handle XS generation are Serpent [9], OpenMC [79], RMC [80], and McCARD [81].

The Serpent project

The vast majority of the results in this thesis was generated by the Serpent computer code. Originally named PSG [82], this code is actively developed and maintained by the VTT Technical Research Centre of Finland. The project began in 2004, and two separate versions of the code exist. Serpent 1 is distributed by the OECD/NEA Data Bank [83] and by the Radiation Safety Information Computational Center (RSICC) [84]. Serpent 2 is in beta-testing phase. Much of the computational efficiency of Serpent is attributable to the Woodcock delta-tracking method [85], and to a unionized energy grid [86]. A dedicated site [87] presents all the features and developmental status of the project. The main applications of Serpent are:

- Spatial homogenization for deterministic codes.
- Fuel cycle studies.
- Validation of deterministic lattice solvers.
- Full-core modeling.
- Coupled multi-physics applications.
- Educational purposes.

A few examples of code sequences where Serpent was applied to few-group XS generation in various reactor types may be found in references [88–92].

2.4.1 Neutron leakage models

In the 2-step approach (Section 2.3), the commonly adopted assumption of identical assemblies constituting an infinite lattice has some impact on the quality of the full-core diffusion calculations, because the use of either reflective or periodic boundary conditions fails to capture the energy-dependent neutron exchange that takes place between a given assembly and its neighbors. This exchange plays an important role in the spatial distribution of pin powers, as well as in the average neutron spectrum inside the assembly.

What follows is the description of some numerical models that can be used in Monte Carlo XS generation in order to correct for the adoption of zero-net-leakage boundary conditions[4]. The treatment of leakage at cell level, however, affects the quality of XS data generated either by deterministic or stochastic techniques.

Homogeneous B_1 corrections

This method was originally developed for deterministic neutron transport solvers. Its main assumption is the factorization of the scalar neutron flux into spatial and energy components. This separability allows a modal expansion of the neutron flux, where each mode satisfies the Helmholtz equation. By solving for the first mode, one obtains a leakage-corrected assembly-averaged spectrum, known as the *fundamental mode flux*, that is used for XS collapsing and for the calculation of diffusion coefficients. The detailed derivation of the method may be found in the work by Stamm'ler and Abbate [28].

The B_1 method has been incorporated into the codes `Serpent` [88] and `McCARD` [81]. Martin and Hébert [93] developed an original adaptation of the method to treat B_1-based leakage as a part of the neutron random walks. It is important to remark that the B_1 method, as implemented in `Serpent`, only corrects the spectral weighting of the XS data and diffusion coefficients, but does not introduce any actual leakage into the system during the transport cycle.

Other authors have also resorted to bucklings as a means of accounting for neutron leakage in MC simulations. These bucklings were obtained either by perturbation theory [94] or by recasting the neutron transport equation in the form of an eigenvalue problem, and subsequently iterating on an axial buckling term [95]. These methods do not resort to homogeneous B_1 corrections.

Albedo iterations

This technique introduces net neutron leakage at assembly level by means of weight modifications upon lattice boundary crossings. The extent of weight adjustments is iterated upon, and depends on how much the infinite lattice model departs from criticality. Yun and Cho [96] developed this technique with special emphasis on the correction of spectral effects during depletion calculations with Monte Carlo.

[4]Periodic boundary conditions result in zero-net-leakage for some symmetric configurations, but not necessarily in the most general case.

Unlike homogeneous B_1 corrections, the use of albedo iterations introduces spatial modifications to the neutron flux, which affect the distribution of pin powers. Whereas Yun and Cho reported on these variations, the effect on few-group XS data generation in a large core with vacuum boundary conditions was not assessed. The albedo method is a promising candidate for the needed simultaneous leakage correction of XS data and discontinuity factors highlighted by Rahnema and Nichita [97]. They referred to this problem as the "leakage assembly environmental effect". The albedo method was implemented in `Serpent` version `2.1.16`.

Layer-expansion leakage model

This novel leakage model was introduced in Publication IV, with a view to develop a heterogeneous scheme where the concept of periodicity was more tangible than in albedo iterations. In order to attain this, the idea of trajectory expansion, or unfolding, was formulated. By means of special indexes, which are updated when a neutron attempts a boundary surface crossing, it is possible to determine the location of that neutron in an expanded system of identical assemblies, as depicted in Fig. 2.2. It is pertinent to point out that trajectories are expanded without resorting to the explicit storage of neighboring assemblies. This results in only modest additional memory overheads.

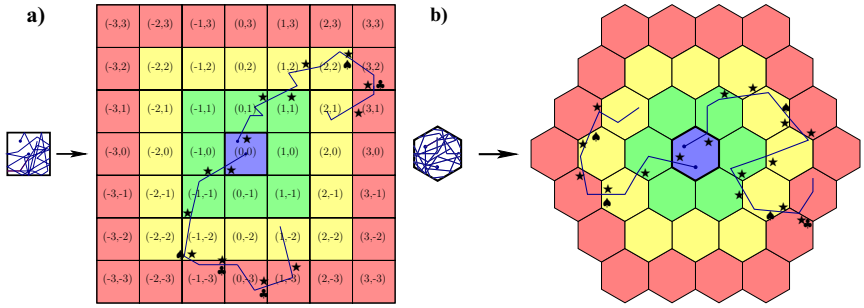

Figure 2.2. Single cell-based and expanded lattice systems used in trajectory unfolding for Cartesian (a) and Hexagonal (b) geometries. Every lattice element corresponds to a heterogeneous assembly. Different colors correspond to different *layers*. Whereas in the case of albedo iterations neutrons undergo weight adjustments upon any surface crossing (indicated by the ★ symbol), in layer-expansion mode the weight is modified only at crossings indicated by the ♠ and ♣ symbols. The layer where these modifications apply is determined by the algorithm in Fig. 2.3 a). Adapted from Publication IV.

Grouping assemblies based on similarity or symmetry considerations leads to the concept of *layers*. The rationale behind the leakage model is to modify the weight of a neutron when it "enters" one specific layer in the expanded

systems of Fig. 2.2. When the neutron attempts to reach a more distant layer, the history is terminated[5]. The determination of the layer index where this happens is the object of the algorithm presented in Fig. 2.3 a), whereas the magnitude of the weight modification is determined by the algorithm in Fig. 2.3 b).

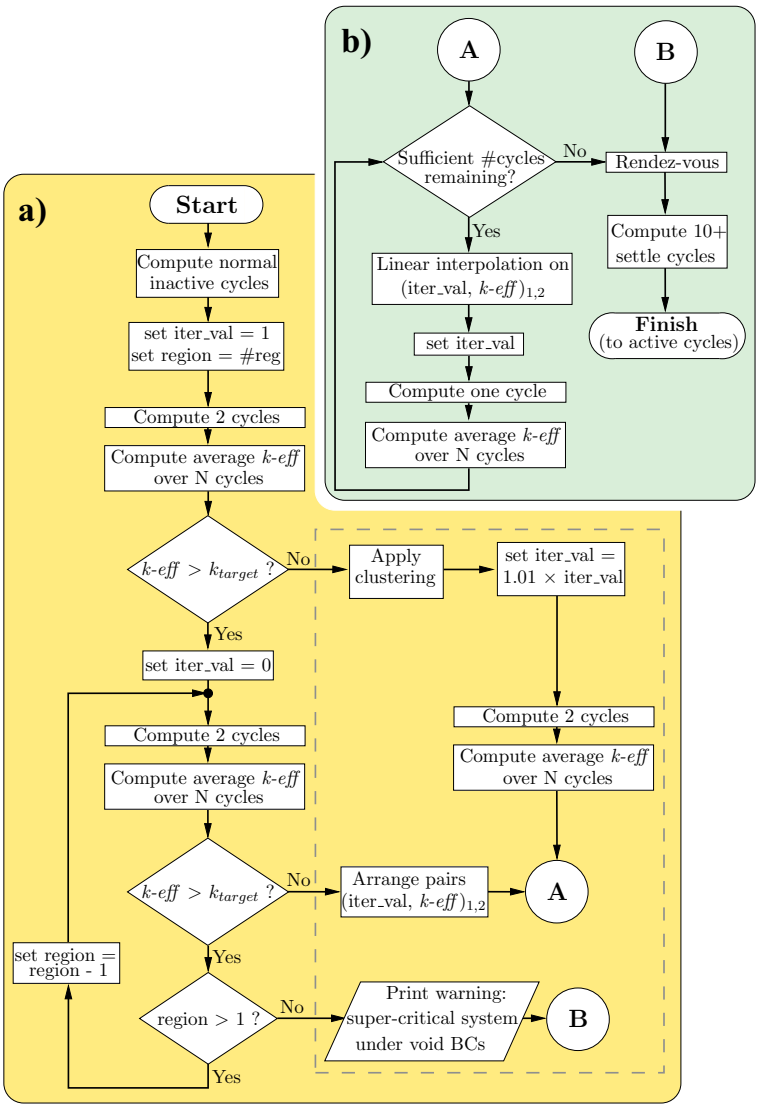

Figure 2.3. Proposed algorithm for the determination of the iteration region index (a) and for the determination of the iteration value, once the region index is known (b). When the algorithm (a) reaches the dashed area, the value of the region is already known. Adapted from Publication IV.

[5]An exception to this applies when the algorithm resorts to *clustering*. When this happens, history termination is substituted by weight modifications, and the layer index is not increased.

The layer-expansion leakage model was preliminarily implemented in the Serpent code version 2.1.21, and requires three input parameters:

1. The desired eigenvalue, k_{target} (generally, 1.0).
2. The maximum number of regions to be used (usually, not more than 4).
3. The number of elements to be averaged (recommended value: 10).

In its lower order form, the layer-expansion leakage model reduces to albedo iterations. This is attained in practice by setting the number of regions to one. When this happens, neutrons are always confined to a single layer, and weight modifications apply at every boundary surface crossing.

2.4.2 Neutron diffusion coefficients

Neutron diffusion coefficients are not a part of the Monte Carlo random walk process, and are therefore not required in the calculations that make use this technique. When Monte Carlo methods are applied to cross section generation, however, a certain diffusion coefficient model is needed. The literature on stochastically generated diffusion coefficients is extensive. Only a few selected methodologies will be described in this thesis.

Definitions based on homogenized transport cross sections
Probably, the simplest method to calculate the diffusion coefficient is to tally the transport cross section, and then make use of Eq. (2.8). In that case, the explicit spatial dependence will no longer hold, because the transport XS will be homogenized. This seemingly straightforward task is not easy to implement in Monte Carlo codes. Referring to Eq. (2.9), the transport correction term can be treated in a variety of ways.

Tohjoh et al. [98] opted for an average of the elastic collision rate extended to all nuclides, and hard-coded constants for the average scattering cosines. Their derivation was limited to three energy groups. Ilas and Rahnema [99] and Redmond [100] proposed and tested modifications to the standard routines in the MCNP code versions 4A and 4B [101]. A homogenized estimate of the transport XS was also one of the implementations used in the first versions of the Serpent code [82]. At a later stage, the treatment of the transport cross section was improved [102] by adapting an in-scatter approximation

via the computation of the flux-weighted inverse transport XS:

$$\Sigma_{tr}^{g} = \frac{\sum\limits_{h \in g} \phi^{h}}{\sum\limits_{h \in g} \frac{\phi^{h}}{\Sigma_{t}^{h} - \overline{\mu}_{0}^{h}\, \Sigma_{s}^{h}}}\,, \tag{2.16}$$

where the index h denotes a micro-group that lies within a given few-group index, identified by g. In an earlier work, Takeda et al. [103] also compared the diffusion coefficients obtained through direct and inverse weighting of the transport XS obtained through deterministic methods.

A new anisotropic formalism

In Publication I, a novel, Monte-Carlo-specific method for the computation of directional diffusion coefficients was proposed. This scheme relies on a special type of score when neutrons traverse a specific surface. The complete derivation of the method may be found in Publications I and II. Here, only the main equations will be introduced. Referring to Fig. 2.4, a neutron that travels from q to p intersects a surface of interest, denoted by $\mathcal{S}$. Diffusion coefficients normal to this surface are computed.

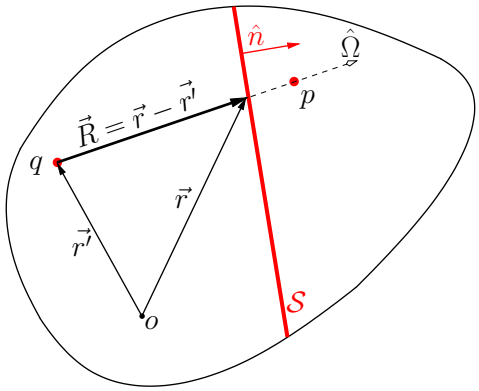

Figure 2.4. Surface crossing variables: the neutron flying from point q to point p intersects the surface $\mathcal{S}$ at the coordinate $\vec{r}$. From Publication II.

Let $\vec{R} = R\,\vec{\Omega}$ be the displacement vector between the source point q (either a fission, fixed, or collision source point) and the crossing point on $\mathcal{S}$. By assuming that this single crossing can be associated with a fixed, isotropic source, simple analytical expressions can be obtained for the scalar flux:

$$\phi(\vec{r}) = \frac{w\, \exp\left(-\int_{0}^{R} \Sigma_{t}(s)\, ds\right)}{4\,\pi\, R^{2}} \tag{2.17}$$

and for the angular current:

$$\vec{J}(\vec{r}) = \frac{w\, \exp\left(-\int_{0}^{R} \Sigma_{t}(s)\, ds\right)}{4\,\pi\, R^{2}}\, \hat{\Omega}\,, \tag{2.18}$$

where w is the neutron weight[6]. The gradient of Eq. (2.17) along the normal $\hat{n}$ takes the form:

$$\frac{\partial \phi(\vec{r})}{\partial n} = -\frac{w \, \exp\left(-\int_0^R \Sigma_t(s)\, ds\right)}{4\,\pi\, R^2} \left(\Sigma_t|_R + \frac{2}{R}\right) \hat{\Omega} \bullet \hat{n}\,. \tag{2.19}$$

By projecting Eq. (2.18) along $\hat{n}$, one obtains the net neutron current due to this surface crossing:

$$J_n(\vec{r}) = \frac{w \, \exp\left(-\int_0^R \Sigma_t(s)\, ds\right)}{4\,\pi\, R^2} \hat{\Omega} \bullet \hat{n}\,. \tag{2.20}$$

In a Monte Carlo sense, one could attempt to apply Fick's law in 1-D by accumulating the quantities from Eqs. (2.20) and (2.19) , and then computing their ratio. This approach was not adopted due to several practical considerations:

- It is possible that similar contributions from different directions cancel out, thus yielding a nearly-zero estimate in Eq. (2.19), which causes numerical problems when computing the quotient. This is particularly troublesome in the case of symmetry planes or reflective boundary conditions. These problems were evident in the method devised by Milgram [104].
- The previous situation can be circumvented by accumulating the necessary quantities in different bins, according to the sense of the surface crossing, and by then averaging the contributions, at the expense of increased complexity.
- The evaluation of the integral attenuation term $\exp\left(-\int_0^R \Sigma_t(s)\, ds\right)$ entails computational overheads.
- The presence of the $1/R^2$ dependence in Eqs. (2.20) and (2.19) poses challenges for small values of R. Such cases would require a special treatment, similar to the evaluation of the scalar flux at a point [105].

In order to avoid these pitfalls, it is possible to compute the ratio[7] of Eqs. (2.20) and (2.19) for every surface crossing, which results in the special score:

$$D_n = \frac{R}{2 + R\ \Sigma_t|_R}\,. \tag{2.21}$$

By following this approach, the resulting "diffusion coefficient" will be unnormalized, since the neutron currents and scalar fluxes are the result of

[6]This quantity is introduced in connection with implicit capture, commonly used in Monte Carlo particle transport.

[7]And change the sign, according to Fick's law.

collective contributions. In Eq. (2.21), $\Sigma_t|_R$ is the total cross section at the crossing point. It is important to highlight that the system under study is heterogeneous. Denoting by $\langle D_n \rangle$ the mean value of the scores D_n, the new method estimates, after normalization, the average total cross section extended to surface $\mathcal{S}$ as:

$$\langle \Sigma_t \rangle = \frac{2\, e^2\, \mathbf{Ei}(-2) + 1}{\langle D_n \rangle} = \frac{\alpha}{\langle D_n \rangle}\,, \tag{2.22}$$

where Ei is the Exponential Integral function. Using tabulated values of Ei (see [106]), one has $\alpha = 0.2773427662$. In Publication I, the normalization procedure was based on the assumptions of an infinite homogeneous medium and isotropic flux, for which the analytical expression of α could be procured. With the relationship of Eq. (2.22), an average transport cross section over $\mathcal{S}$ can be estimated:

$$\langle \Sigma_{tr} \rangle = \frac{\alpha}{\langle D_n \rangle} - \overline{\mu}_0\ \langle \Sigma_s \rangle\ , \tag{2.23}$$

where the energy indexes were dropped for simplicity. $\overline{\mu}_0$ is the cell-averaged mean scattering cosine. In Publication I, $\langle \Sigma_s \rangle$ was taken as the homogenized, flux-and-volume-weighted scattering cross section. Thanks to the insights gained during that work, the averaged transport XS in Publication II was further modified in order to include a problem-dependent interpolation constant m, as well as the total-current-weighted scattering and total cross sections:

$$\langle \Sigma_{tr} \rangle\ |_{\mathbb{J}} = \ (1-m)\ \frac{\alpha}{\langle D_n \rangle}\ +\ m\ \langle \Sigma_t \rangle\ |_{\mathbb{J}}\ -\ \overline{\mu}_0\ \langle \Sigma_s \rangle\ |_{\mathbb{J}}\ , \quad 0 \leq m \leq 1\,. \tag{2.24}$$

Eventually, the resulting transport cross section is also current-weighted, as denoted by the $|_{\mathbb{J}}$ identifiers. The introduction of the interpolation constant m also aims at correcting for the assumptions of infinite homogeneous medium and isotropic flux postulated in the derivation of α in Eq. (2.22).

The aim of the new method is to obtain a diffusion coefficient by substitution of the transport XS (obtained either through Eqs. (2.23) or (2.24)) into Eq. (2.8).

A note on directional averages is due: in Publication II, only axial directional diffusion coefficients (D_Z) could be calculated with the new formalism as implemented in `Serpent`. In order to account for the radial direction, an approximation previously used by Gho [107] in the `HETAIRE` [108] cell code was adopted. Namely, the radial diffusion coefficient (D_R) was derived from the isotropic –standard– diffusion coefficient (D_{std}) calculated by `Serpent`, and the axial diffusion coefficient D_Z:

$$D_R = \frac{1}{2}(3\, D_{std} - D_Z)\,. \tag{2.25}$$

At a later stage, a mesh-based averaging technique was introduced in Publication III. This will be illustrated in Section 3.2.

From B_1 equations

As described in Section 2.4.1, the homogeneous B_1 leakage model also supplies few-group diffusion coefficients collapsed with the criticality spectrum. Monte Carlo codes such as `McCARD` and `Serpent` incorporate this functionality.

Milgram's method

A work by Milgram [104] takes a different approach towards the calculation of axial diffusion coefficients in a CANDU[8] reactor cell, since no attempt is made to calculate any transport cross section, and therefore Eq. (2.8) is not needed altogether. Instead, Milgram proposes a functional fit of Fick's law (Eq. (2.7)) through numerous axial-dependent estimators of the net neutron currents and scalar fluxes in three energy groups. As a result, diffusion coefficients are obtained by post-processing quantities tallied during the Monte Carlo simulations carried out with `MCNP`. A schematic representation of the calculation domain and diffusion coefficients is presented in Fig. 2.5.

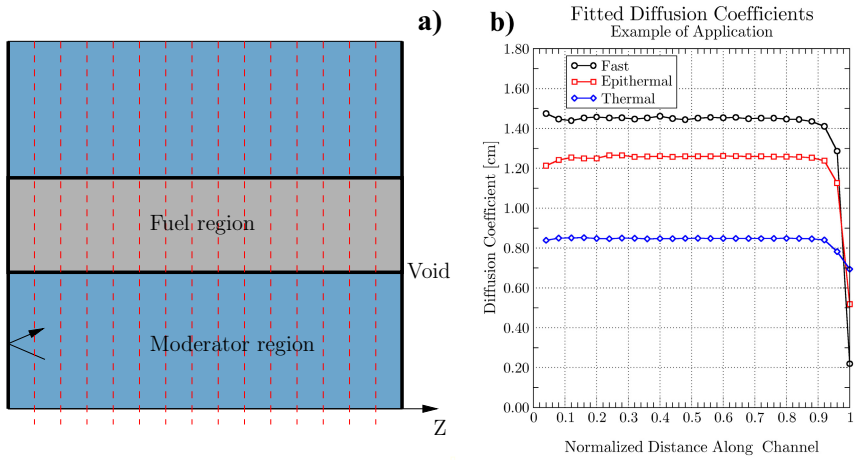

Figure 2.5. An illustration of Milgram's method applied to the axial direction. Schematic domain (a) with dashed vertical lines indicating tallying surfaces and mesh extents for scalar flux calculations. Reflective boundary conditions are applied at the left boundary and in the X–Y plane. In (b), an example calculation of 3-group diffusion coefficients. For illustrative purposes only.

The system under consideration must have leakage, so that the net neutron current in Eq. (2.7) does not vanish, as occurs at reflective boundaries. Milgram conducted a meticulous study on the assumption of flux factorizabil-

[8]CANDU® (CANada Deuterium Uranium®)

ity and on the applicability of diffusion theory, as well as on the implications of different channel lengths and fitting techniques on the diffusion coefficient statistics.

The application of Milgram's method to few-group XS generation is not straightforward, due to statistical considerations, but primarily due to the need for neutron leakage, and the criteria for the rejection of estimates at locations where the diffusion approach is not valid. In spite of this, the method can be a valuable tool for the comparison of different diffusion coefficient formalisms. Van Rooijen et al. [109] applied the method to the calculation of anisotropic diffusion coefficients with the `MVP` computer code [110], and readily identified the need to report results in the form of confidence intervals. Van Rooijen and Chiba [111] compared the diffusion coefficients obtained by Monte Carlo techniques and by the (deterministic) Method of Characteristics, and concluded that the stochastic approach entailed prohibitive running times.

Other methods

This overview of methods would be far from complete if the works by Gelbard and Pego [112], Gast [113] and Yamamoto [114] were not mentioned. In the first of these works, the authors postulate a buckling-based expansion of the neutron source in an infinite lattice configuration, and implement an elaborate algorithm involving "real" and "image" neutrons. Gast compared results obtained through different formalisms, and proposed an empirical correction factor for the fast energy range. In his work, he points out that the transport cross section should be current-weighted. Yamamoto addresses the simultaneous leakage-correction of XS data and generation of anisotropic diffusion coefficients via the introduction of complex neutron weights in the Monte Carlo random walks.

In the early years, computational constraints drove most works on deterministic and stochastic diffusion coefficients generation to be limited to comparisons against formalisms, thus not assessing the performance of these formalisms on full-core diffusion calculations. Pertaining diffusion coefficients procured by Monte Carlo techniques, Yamamoto's view [95] is that:

> "the methods are considered unverified and not necessarily recommended to be used for group constant generation."

2.4.3 Discontinuity factors

At cell level, zero-net-current conditions in all boundaries allow the adoption of the volume-averaged heterogeneous flux as a replacement for the surface-averaged homogeneous flux needed in Eq. (2.14). Under these conditions, the computation of discontinuity factors by Monte Carlo codes does not pose major challenges. Tohjoh et al. [98] applied this infinite medium approach to the generation of boiling water reactor (BWR) cross section data. The Serpent code also has built-in capabilities for the computation of 2-D discontinuity factors.

When non-zero leakage exists at any of the assembly boundaries, it is necessary to estimate the surface-averaged homogeneous flux at cell level by using a (deterministic) diffusion solver. Examples of this are available for 1-D radial [115], 1-D axial [116, 117], and 2-D radial [90] problems. In all of these works, the computation of homogeneous fluxes was carried via post-processing Serpent results with the help of dedicated tools[9]. Cho and Lee [118] also generated 2-D leakage-corrected discontinuity factors, but it is unclear if the homogeneous fluxes were or were not calculated in line with the Monte Carlo computations.

The examples cited so far apply to light water reactors, with the exception of the works by Fridman et al. [116] and by Hall et al. [117], which apply to hard-spectrum, high conversion BWR cores. In high-temperature, gas-cooled reactors, Zika and Downar [119] identified numerical divergences when applying discontinuity factors. Although Yamamoto [120] later proposed means of overcoming the divergences, it is of interest to test the performance of anisotropic diffusion coefficients in scenarios where the application of Equivalence Theory is not straightforward, as well as to attempt to generate 3-D discontinuity factors for other reactor types, such as SFRs.

In Publication III, the implementation of a finite-difference-based diffusion solver into Serpent is described. This routine allows the calculation of 3-D leakage-corrected discontinuity factors in line with the transport cycle. This is advantageous not only for simplicity, but also because statistical uncertainties can be assigned to all generated few-group constants.

[9] Shortly after the publication of the work by Leppänen et al. [90], a 2-D homogeneous flux solver based on analytical function expansion was incorporated into Serpent version 2.1.22. The solver can be used for the calculation of radial, leakage-corrected discontinuity factors and for pin power reconstruction.

3. Neutron diffusion coefficients in Monte Carlo

The generation of few-group neutron diffusion coefficients to be used in core calculations is demanding for deterministic as well as for stochastic neutron transport solvers. The challenge resides in that diffusion coefficients, contrarily to other XS data, cannot be calculated through a mere preservation of reaction rates.

Lattice-level calculations have been historically dominated by deterministic methods. Along with the progress in computational power and parallelization, Monte Carlo techniques have found increased application in assembly calculations. The preservation of multi-group reaction rates in the original (heterogeneous) infinite lattice transport problem and in the resulting (homogenized) system dictates the adoption of a flux-and-volume XS weighting schemes.

As for diffusion coefficients, different formalisms were implemented in MC assembly codes, mostly as a result of the various methods previously implemented in deterministic codes. Equivalence Theory allows some flexibility in the definition of the diffusion coefficients. Rahnema and Nichita [97] make explicit mention of the arbitrariness in the diffusion coefficient definition. To this, Cho [35] adds that:

> "in modern nodal methods . . . the direction dependency of the diffusion coefficient can be ignored and the diffusion coefficient itself can be determined arbitrarily (conveniently for practice) according to the equivalence theory for homogenization. But the burden is transfered to the discontinuity factors."

In cases where discontinuity factors are not used, however, it is expected that the way in which the diffusion coefficients are defined will impact the quality of core-level results.

This chapter will first address a study on some basic properties of the dif-

fusion coefficients generated by Monte Carlo techniques based on Eq. (2.8). The study will be supported with findings from Publication I. Later on, more refined 3-D models will be used for the generation of diffusion coefficients in a fast reactor system. These coefficients will be compared, and their performance in full-core diffusion calculations will be assessed, making use of selected results from Publications II and III. A study on the applicability to other reactor types will also be presented, followed by core calculations of a CANDU reactor, reported in Publication V.

3.1 Diffusion coefficients: on their functional dependence

Prior to the analysis of realistic full-core problems, it is pertinent to examine some basic properties of the diffusion coefficient models. Publication I is dedicated to the comparison of three Monte-Carlo-based diffusion coefficient generation methods in one spatial dimension, with special emphasis on some properties of the newly proposed technique described in Section 2.4.2. Whereas the first two methods scrutinized are based on Eq. (2.8), they differ in how the transport cross section is defined. The third method was introduced for comparison purposes. Originally proposed by Milgram [104], this scheme is free from the assumptions of lattice theory.

The calculations were conducted with a multi-group MC code specifically developed for Publication I. The diffusion coefficients compared are denoted by D_{tr}, D_J, and D_{fit}. The models used to compute them are based on:

D_{tr}: a flux-and-volume-weighted homogenized transport cross section, Σ_{tr}, and the use of Eq. (2.8). This method was in use by the `Serpent 1` code [82]. Shortly after Publication I was presented, another method that superseded the former was implemented in `Serpent 2` [102].

D_J: the novel methodology for the estimation of the total cross section, Σ_t, derived in Section 2.4.2. By adding the flux-and-volume weighted transport correction term, the transport cross section of Eq. (2.23) is obtained. This, in turn, is applied to the calculation of diffusion coefficients through Eq. (2.8).

D_{fit}: the method proposed by Milgram [104]. This scheme aims at providing a functional fit to Fick's law (Eq. (2.7)), without resorting to the transport cross section. Milgram's approach does not lend itself to the calculation of "benchmark" values. On this, van Rooijen and Chiba [111] state that only "best-estimate" values could be expected. For compari-

son purposes, however, this method is advantageous in that it allows a certain degree of parametrization of Fick's law by means of the XS set supplied to the multi-group MC solver. This parametrization is then exploited to test the ability of Eq. (2.8) to capture functional dependences.

Under the assumption of linearly anisotropic scattering in a homogeneous medium, the one-group results of Fig. 3.1 reveal that both diffusion coefficients D_{tr} and D_J undergo similar trends as a function of the mean scattering cosine in the laboratory reference frame. D_{tr} values, however, have no dependence with the optical thickness of the medium, whereas D_J values do exhibit variations which improve the agreement with the best-estimates from Milgram's formalism (D_{fit}) for optically thin[1] media. Pertaining the latter formalism, it is important to highlight that the associated statistical uncertainties are prohibitively large.

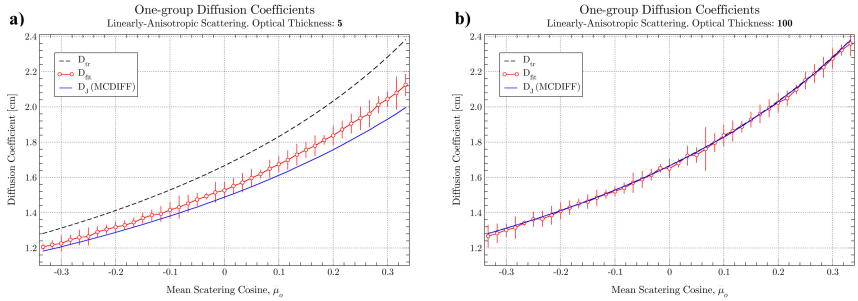

Figure 3.1. Linearly anisotropic one-group diffusion coefficients for optically thin (a) and thick (b) media. Optical thicknesses are expressed in units of mean free paths (mfp). Results obtained through Milgram's method are represented as 95% confidence intervals. Other models include one standard deviation error bars. Adapted from Publication I.

Thus far, the attention has been focused on linearly anisotropic scattering laws. Other scattering laws (see Fig. 3.2) were also postulated. All these laws can be exactly represented by Legendre polynomials of order 5 or less, and share the same total cross section and average scattering cosine. The results of Table 3.1 show that there is no appreciable difference in D_J coefficients with the scattering law, thus indicating that the transport correction of order 0 is sufficient at this level of accuracy. The accuracy is dictated by the poor statistical quality of the estimates provided by Milgram's method.

[1] A thickness of 5 mpf is insufficient for diffusion theory to hold, given the vacuum boundary conditions. This scenario was selected as a limiting case where Milgram's method yields values that depart significantly from the asymptotic, infinite medium solution.

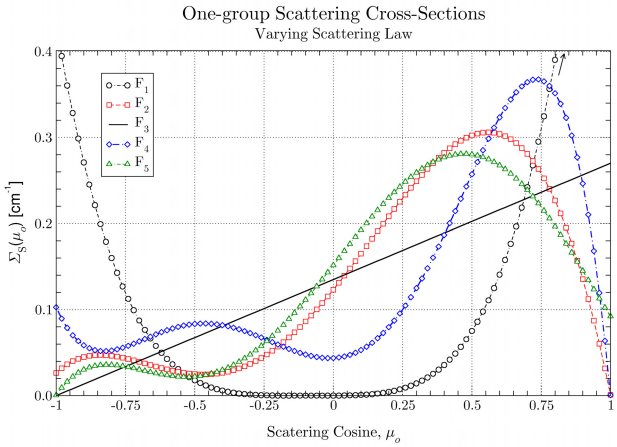

Figure 3.2. Scattering laws used for one-group diffusion coefficient calculations. All laws can be represented by Legendre polynomials of order 5 or less. $\overline{\mu}_0 = 0.3333$. $\Sigma_0 = 0.27\,cm^{-1}$. Results from Publication I.

Table 3.1. Diffusion coefficients for varying scattering laws. Optical thickness: 30 mfp.

Scattering	Diffusion Coefficients (cm)			
Law	D_{tr}	D_J	$\Delta_{D_J}\|_{1\sigma}$	D_{fit} (95 % CI)
F_1	1.58723	1.5734	0.0005	(1.560 – 1.591)
F_2	1.58723	1.5737	0.0008	(1.575 – 1.590)
F_3	1.58723	1.5734	0.0005	(1.573 – 1.589)
F_4	1.58723	1.5742	0.0010	(1.572 – 1.589)
F_5	1.58723	1.5735	0.0005	(1.574 – 1.589)

3.2 3-D systems

The simplistic nature of the homogeneous, one-dimensional models studied in Publication I was adequate for a first introduction to the properties of the new directional diffusion coefficient model. However, the limitations of its implementation hampered any application to realistic problems.

In Publication II, the transport cross section of Eq. (2.23) was modified in two ways. The first change was to use the neutron-current-averaged scattering XS, $\langle \Sigma_s \rangle |_{\mathbb{J}}$. The second one was the introduction of an interpolation constant m and the neutron-current-averaged total cross section, $\langle \Sigma_t \rangle |_{\mathbb{J}}$.

The final expression of the transport cross section is given by Eq. (2.24). The new directional diffusion coefficient formalism was preliminarily implemented in the code `Serpent 2`, and limited to the axial direction only. This limitation entailed making use of Eq. (2.25).

A sensitivity study was conducted in order to optimize the interpolation

constant m in Eq. (2.24) for sodium-cooled fast reactor studies. A value $m = 0.85$ was found to furnish good agreement for normal and coolant voided conditions.

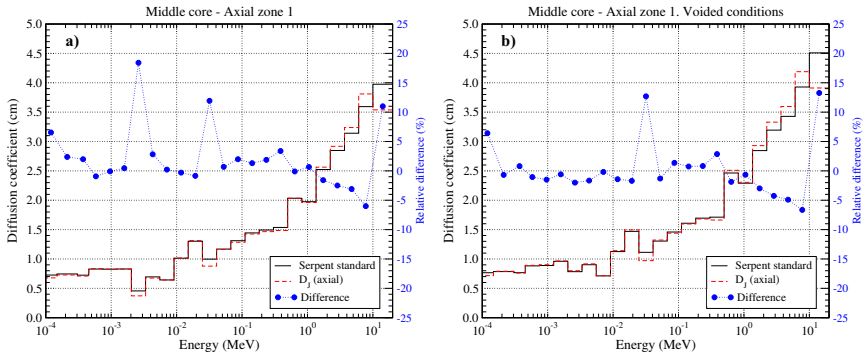

Figure 3.3. A comparison between Serpent's standard –isotropic– and directional axial diffusion coefficients in an SFR cell for normal (a) and coolant voided (b) conditions. Relative differences are reported in the right axis. Adapted from Publication II.

Fig. 3.3 presents a comparison of diffusion coefficient results. The extent of anisotropy is significant in a few energy groups only. In Fig. 3.3 a), the presence of sodium is responsible for the first peak in the relative differences between isotropic and axial diffusion coefficients. This is attributable to the 2.805 keV absorption resonance of ^{23}Na. Under normal operating conditions, neutrons streaming in the axial direction around this energy are more likely to leak through the fuel than through the coolant. When the coolant is voided, axial streaming is increased.

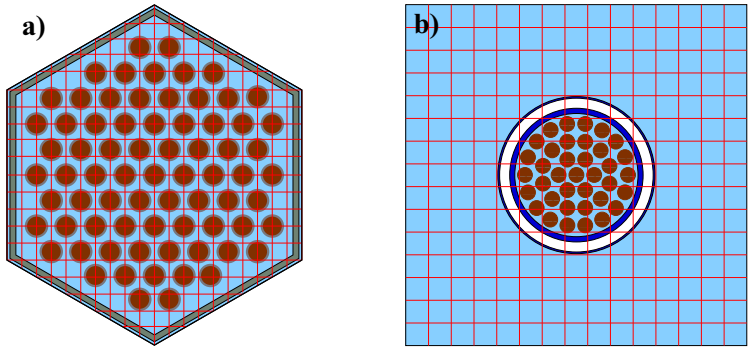

Figure 3.4. A regular superimposed Cartesian mesh for the simultaneous treatment of diffusion coefficient scores per direction in hexagonal (a) and square (b) cells.

Using Eq. (2.25) implies that some of the properties of the isotropic diffusion coefficients are retained, which is undesirable. In Publication III, the limitation to generate anisotropic diffusion coefficients only along the axial

direction was overcome by means of a superimposed regular Cartesian mesh, illustrated in Fig. 3.4. With the help of this mesh, radial diffusion coefficients could be generated.

In Fig. 3.5, the differences between the radial and the axial components of the diffusion coefficients in a control rod (CR) are strongly energy-dependent, and can be as large as 25%. Considerably larger differences can be expected, nevertheless, between the standard and directional diffusion coefficient formalisms.

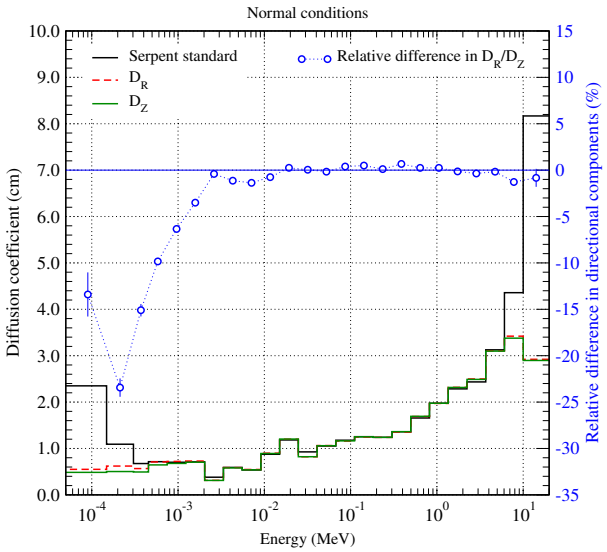

Figure 3.5. Radial (D_R) and axial (D_Z) directional coefficients in an SFR control rod assembly and comparison against standard diffusion coefficients. From Publication III.

3.3 Application to neutron diffusion calculations in a fast reactor

Thus far, diffusion coefficients obtained by different methods were compared. In themselves, such comparisons do not yield any conclusive information about the convenience of opting for a given formalism. To that end, it is necessary to perform full-core diffusion calculations and contrast those solutions against reference values. This section reports on the performance of diffusion coefficient generation methods when few-group cross section data sets calculated by `Serpent 2` are fed to a diffusion solver.

The use of the same Monte Carlo code and associated cross section data library for the generation of a reference full-core solution as well as of few-group XS data is greatly advantageous for comparison purposes against dif-

fusion results. In Publications II and III, the two-step calculation procedure was applied to the study of a medium-sized Advanced Burner Reactor (ABR) with oxide fuel at Beginning of Cycle (BOC) conditions.

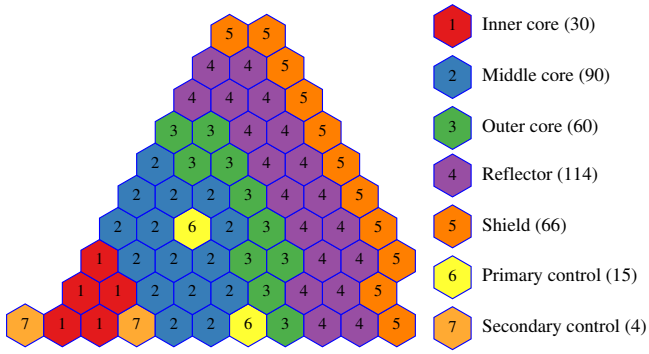

Figure 3.6. Top view of the oxide core version of the ABR benchmark problem with 1/6 periodic symmetry. Heterogeneous assemblies are schematically depicted as solid regions. Primary and secondary control rod banks were not discriminated in the cases under study. From Publication III.

The detailed ABR benchmark specification is described in the report by Blanchet et al. [121]. Fig. 3.6 provides a schematic top view of the ABR core. In the axial direction, the system is heterogeneous. From top to bottom, all the elements listed in Table 3.2 are present in the fuel sub-assemblies.

Table 3.2. Axial configuration of a driver sub-assembly in the ABR oxide core. The same definition applies to the Inner, Middle and Outer elements. Radial sub-assembly pitch: 16.2471 cm. Number of fuel pins: 271. Based on Blanchet et al. [121].

Element name	Axial length (cm)
Upper structure	44.70
Gas plenum	172.41
Zone 5	22.988
Zone 4	22.988
Zone 3	22.988
Zone 2	22.988
Zone 1	22.988
Lower reflector	112.39
Lower structure	35.76

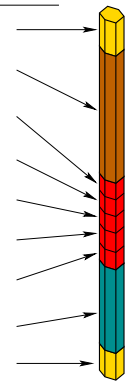

During the XS generation process, different approaches were adopted in Publication II to account for neutron leakage at assembly level. Since the relative performance of leakage models will be scrutinized in Chapter 4, here the reporting is based on results obtained using the so-called *axially hetero-*

geneous models with 24 energy groups[2].

An axially heterogeneous model includes all the components listed in Table 3.2. Pertaining boundary conditions, axial vacuum and radial periodicity were used. It is worthwhile highlighting that these XS generation models are intrinsically three-dimensional and can be represented without difficulties in Serpent. As a result, few-group XS data sets for every axial region is obtained.

3.3.1 Un-rodded system

In Publication II, the new anisotropic diffusion formalism was applied for the first time to a 3-D heterogeneous core. Control rods were not modeled for simplicity. Instead, they were replaced by sodium-filled regions.

The performance of the diffusion coefficient models was assessed in terms of system eigenvalue, axial and radial power profiles against reference Monte Carlo results. Table 3.3 compares extrapolated diffusion results obtained with the TRIZ computer code [11] for normal and coolant voided conditions. With the exception of the radial power distribution, for which maximum discrepancies with reference results do not exceed 1%, anisotropic diffusion coefficients clearly improve the quality of the diffusion solutions.

Table 3.3. Summary of 3-D results for the ABR core without control rods. For normal conditions, the reference eigenvalue obtained with Serpent is *k-eff* $= 1.03732 \pm 0.00001$. For voided conditions, *k-eff* $= 1.05620 \pm 0.00001$.

Coolant conditions	Model for D	*k-eff*	$\Delta\rho$ (pcm)	$\Delta^{max}_{Pow}\vert_Z$ (%)	$\Delta^{max}_{Pow}\vert_R$ (%)
normal	standard	1.03317	-387	2.61	0.73
	anisotropic	1.03607	-116	1.23	0.95
voided	standard	1.05355	-238	1.92	0.89
	anisotropic	1.05612	-7	1.47	0.81

$\Delta^{max}_{Pow}\vert_Z$: maximum relative difference in axial power distribution.

$\Delta^{max}_{Pow}\vert_R$: maximum relative difference in radial power distribution.

Figure of merit

The choice of an optimal calculation scheme generally arises from a trade-off between the accuracy of the solution and the computational resources

[2] The group structure used is partially based on the ECCO-33 [122] structure used in the ERANOS [5] code system. Following considerations from Fridman and Shwageraus [89], the lowest-energy groups were merged until a total of 24 groups was attained. The resulting structure is presented in Table 4.1.

needed. In an attempt to quantify the efficiency of the two-step approach, a Figure of Merit (FOM) was defined:

$$\text{FOM} \equiv \frac{1}{|\Delta_k|\ T}\,, \tag{3.1}$$

where $|\Delta_k|$ is the absolute error in *k-eff*, and T is the total[3] computation time. Eq. (3.1) results in larger values for solutions that entail high accuracy, or which require short computer times. The definition of a FOM is not unique[4]. The form proposed here pursues a simplistic, straightforward means of comparison, since it does not cater for memory requirements nor errors in the power distributions. Through Eq. (3.1), it is possible to calculate FOMs for the cases reported in Table 3.3, as well as to compare such values against the figure of merit obtained through full-core Monte Carlo calculations.

Table 3.4. Computational figure of merit comparison between full-core Monte Carlo and the 2-step scheme, via Eq. (3.1). For the full-core Monte Carlo case, $|\Delta_k|$ is the statistical uncertainty reported by Serpent. For the 2-step approach, $|\Delta_k|$ is the difference against MC results, and also includes a bias of 13 pcm due to the statistical nature of the XS, as discussed in Publication II. Memory use –not considered in Eq. (3.1)– and CPU times are unpublished results from the same calculations.

Coolant conditions	Scheme	Model for D	Memory (MB)	$\lvert\Delta_k\rvert$	T (min)	FOM
normal	MC	n/a	6938	0.00001	59592	1.68
	2-step	standard	5600	0.00428	1811	0.13
	2-step	anisotropic	5600	0.00138	1818	0.40
voided	MC	n/a	6938	0.00001	63624	1.57
	2-step	standard	5600	0.00278	1823	0.20
	2-step	anisotropic	5600	0.00021	1827	2.61

The results of Table 3.4 highlight the large computation times taken by the full-core MC solutions, which would be inviable without parallelization techniques. In the 2-step approach, the vast majority of the time is taken by the XS generation step.

For normal conditions, anisotropic diffusion coefficients outperform standard diffusion coefficients due to increased accuracy, whilst the computational overheads are very similar[5]. The full-core MC approach has a higher

[3] In the case of parallel calculations, this is the direct sum of the times per task.

[4] In the MCNP code [71], the relative error of a tally, R, is introduced, and the FOM is defined as $1/(R^2\,T)$. In connection with Eq. (2.15), this figure of merit should be approximately constant, and is used both as a tally convergence indicator and as a measure of variance reduction techniques' performance.

[5] The computational time of the standard diffusion coefficients is being penalized by around 20 %, due to the implementation of the anisotropic routine in Serpent.

FOM, but this value would decrease if the inter-cycle bias was properly assessed. For voided conditions, the anisotropic diffusion formalism in the 2-step approach has the best performance.

The FOM values reported in Table 3.4 fail to put in evidence the enormous versatility of the 2-step approach: by using the same preexisting XS sets, various reactor configurations can be studied via inexpensive diffusion runs. Conversely, the full-core Monte Carlo approach would entail several time-consuming calculations, which might necessitate large, expensive computing facilities.

3.3.2 Rodded system

In Publication III, control rods were incorporated into the ABR system. Modeling strong absorbers in diffusion theory is challenging, mainly because the validity of Eq. (2.4) is breached. It is unlikely that a mere *ad hoc* re-definition of the diffusion coefficients can circumvent the inapplicability of diffusion theory. Amid the alternatives available to lessen the effect of this limitation, the following were tested:

- Discontinuity factors.
- Internal boundary conditions (IBCs).

The computation of 3-D discontinuity factors required modifications to the preexisting routines available in `Serpent`. The first one entailed extensions to tally heterogeneous neutron fluxes and partial neutron currents in the axial direction, whereas the second one was the implementation of a mesh-centered, finite-difference diffusion solver for the computation of leakage-corrected discontinuity factors. The choice of finite differences followed the need for consistence with the solver `TRIZ`. Herrero et al. [123], for example, emphasize the importance of this consistence.

Internal boundary conditions were typically used in thermal reactor analysis, as in the works by Bretscher [124], by Bretscher et al. [125], and in the `HEXTRAN` code [126]. IBCs are input to the diffusion solver in the form of multi-group current-to-flux ratios at control rod locations[6]. These regions are then excluded from the computational domain. This technique resulted advantageous due to its simple implementation in the diffusion solver `TRIZ`, and because face-averaged fluxes and neutron currents were readily avail-

[6]Depending on the particular application, IBCs can also be applied at reflectors.

able from the computation of DFs.

An overall poor performance of the standard diffusion coefficient model without corrections is evident from the results of Table 3.5. For the same case, there is a pronounced radial tilt in the powers, as illustrated in the two-dimensional power comparison of Fig. 3.7 a). From Table 3.5 and Fig. 3.7, it follows that the use of anisotropic diffusion coefficients yields the best agreement in radial powers against reference transport values.

Table 3.5. Summary of 3-D results for the ABR core with control rods in withdrawn position. Reference eigenvalue form Serpent: *k-eff* $= 1.02914 \pm 0.00001$.

Model for D	Control rod treatment	*k-eff*	$\Delta\rho$ (pcm)	$\Delta^{max}_{Pow}\vert_Z$ (%)	$\Delta^{max}_{Pow}\vert_R$ (%)
standard	Standard	1.02070	-804	5.28	4.81
	DFs	1.03017	+97	1.88	2.28
anisotropic	Anisotropic	1.02862	-49	4.85	1.27
	IBCs	1.03024	+104	0.97	1.31

$\Delta^{max}_{Pow}\vert_Z$: maximum relative difference in axial power distribution.

$\Delta^{max}_{Pow}\vert_R$: maximum relative difference in radial power distribution.

The introduction of discontinuity factors improved all performance indicators. Nevertheless, certain limitations and pitfalls in the XS generation process have downplayed the extent of ameliorations. It is important to bear in mind that the axially heterogeneous models described in Section 3.3 have no net radial leakage. Also, dedicated discontinuity factors were not generated for fuel sub-assemblies surrounding control rods, thus forfeiting corrections there. Finally, the calculation of homogeneous fluxes in reflector and empty (sodium-filled) control rod positions resulted in negative fluxes. Loberg et al. [127] experienced similar difficulties in light water reactor analyses.

Notwithstanding the improvement brought about by anisotropic diffusion coefficients, the presence of withdrawn control rods significantly deteriorates the axial power distributions. The introduction of discontinuity factors is beneficial, but the adoption of internal boundary conditions improves the quality of the axial distribution further, as can be observed in Fig. 3.8 a).

The drawback posed by the lack of radial leakage-corrected discontinuity factors is apparent in the results of Table 3.6. In a voided scenario, neutrons travel longer distances, thus leakage corrections are expected to be more prominent. Of all the options studied, anisotropic diffusion coefficients with IBCs gave the best agreement in control rod worth.

The control rod S-curves of Fig. 3.8 b) suggest that the quality of IBC

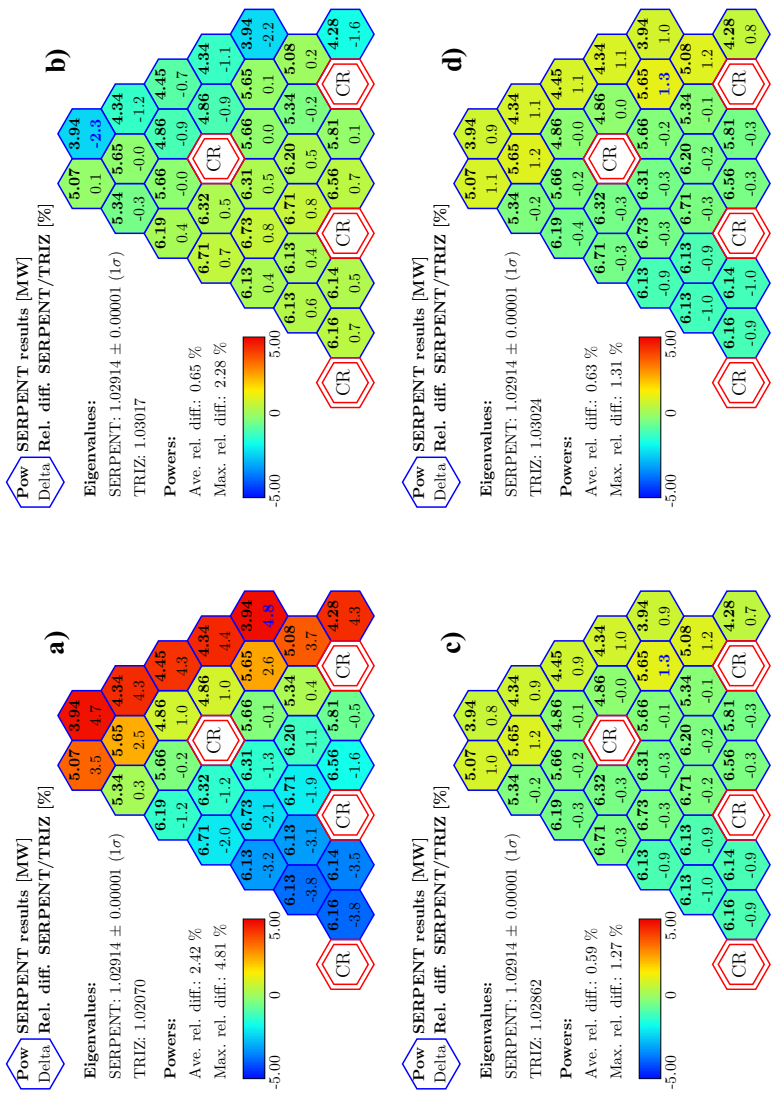

Figure 3.7. Radial assembly power comparison between Monte Carlo and diffusion calculations in 24 energy groups. Control rods are withdrawn. **UDF**: standard diffusion coefficients + unity discontinuity factors (a). **DF**: standard diffusion coefficients + discontinuity factors (b). **ANI**: anisotropic diffusion coefficients (c). **IBC**: similar to **ANI**, with control rods replaced by internal boundary conditions (d). Adapted from Publication III.

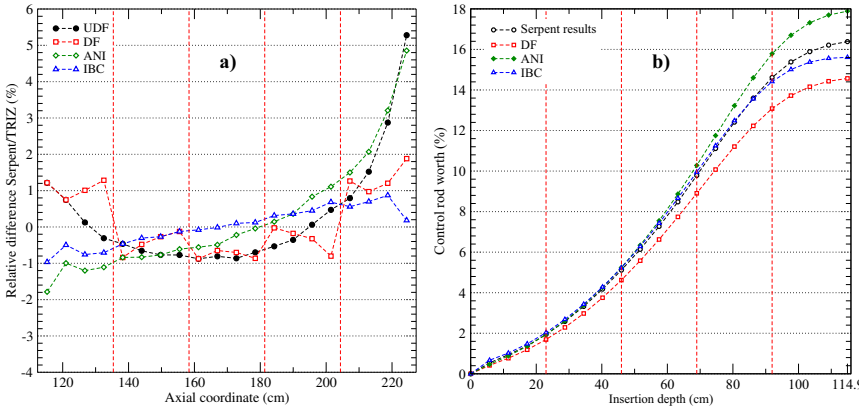

Figure 3.8. Axial power comparisons against the Monte Carlo reference when control rods are withdrawn (a), and control rod worth curves (b). Vertical dashed lines identify fuel zone interfaces. The methods used are indicated by legends which follow the same nomenclature of Fig. 3.7. Adapted from Publication III.

Table 3.6. Sodium void reactivity and control rod worth, calculated as $\left[\frac{\Delta_k}{k}\right]$. Uncertainties are below 0.01 %. Serpent reference values are, respectively, 1.68 and 16.49.

Model for D	DFs?	Control rod treatment	Sodium void worth (%)	CR worth (%)
standard	No	Standard	1.69	17.95
	Yes	DFs	1.88	14.57
anisotropic	No	Anisotropic	1.60	17.89
	No	Internal BC	1.62	15.61

results could be improved even further by a more meticulous treatment of the current-to-flux ratios at the end of the insertion depth (Zone 1 in Table 3.2).

Whilst the introduction of directional diffusion coefficients improved the quality of the diffusion solution, it is fair to question the need for anisotropic constants in virtue of physical considerations. In the past, Shirakata and Iijima [128] conducted experiments on plate-type critical assemblies. As a result, they were able to measure the change in reactivity associated with the rotation of a fuel element. They used this result as a means of validating Benoist's formula [36]. In the case of Pebble-Bed High-Temperature Gas-Cooled reactors, Gerwin and Scherer [129] developed a directional formalism for cylindrical void regions.

Although geometrical and material arguments allow a preliminarily indication on the direction dependence of the neutron streaming process, the presence of structural components and other non-multiplicative regions, such as control rods, makes it difficult to provide a final statement on the sever-

ity of the anisotropy and the consequent need for directional constants. The new formalism described in this thesis is advantageous in the sense that it always provides directional constants. The degree of anisotropy among the components is given by the physics of the problem at the lattice level. In consequence, there is no need to resort to *ad hoc* considerations.

3.4 Extension to other reactor types

Directional diffusion coefficients applied to a fast reactor problem furnished better eigenvalues and power distributions than standard diffusion coefficients. It is of interest to study the performance of anisotropic diffusion constants in other reactor systems. To that end, the first step is to determine an optimal value of the interpolation constant m in Eq. (2.24) by means of combined Monte Carlo and diffusion methods.

In Publication V, a series of tests was conducted on CANDU, Russian-type VVER-440 and prismatic, high-temperature, graphite-moderated gas-cooled reactor (HTR) cells. SFR cells were considered, too, in order to compare results against previous findings from Publication II.

For every reactor design, one-dimensional axial models were used for XS generation with `Serpent 2`. Next, the resulting data was input to the diffusion solver `TRIVAC` [12]. In Fig. 3.9, the results of this study are parametrized with the height of the axial model. With the exception of the SFR cases, calculations were carried using a coarse two-group energy structure, with a cutoff at 0.625 eV, and a relatively fine 23-group structure from the `CASMO` code [22]. Using an iterative procedure for the rejection of outliers described in Publication V, 95% confidence intervals of the optimal interpolation constant per case were established and summarized in Table 3.7.

The effect of group collapsing is severe for the VVER reactor case, and originates a substantial shift in the curves of Fig. 3.9. There is no value of m in the interval $[0, 1]$ that yields equivalence in *k-eff* for this type of cell. Although an intermediate group structure that does yield equivalence could exist, the anisotropic diffusion coefficient formalism is not recommended for light water reactor calculations at this stage.

For the CANDU case[7], optimal interpolation constants for 23 and for 2 energy groups could be determined, albeit the spread in the latter structure

[7] In the CANDU cell, the term "axial" was must be interpreted in the same context as Milgram [104] has used it, i.e., along the fuel channel, which is actually horizontal in this type of reactors.

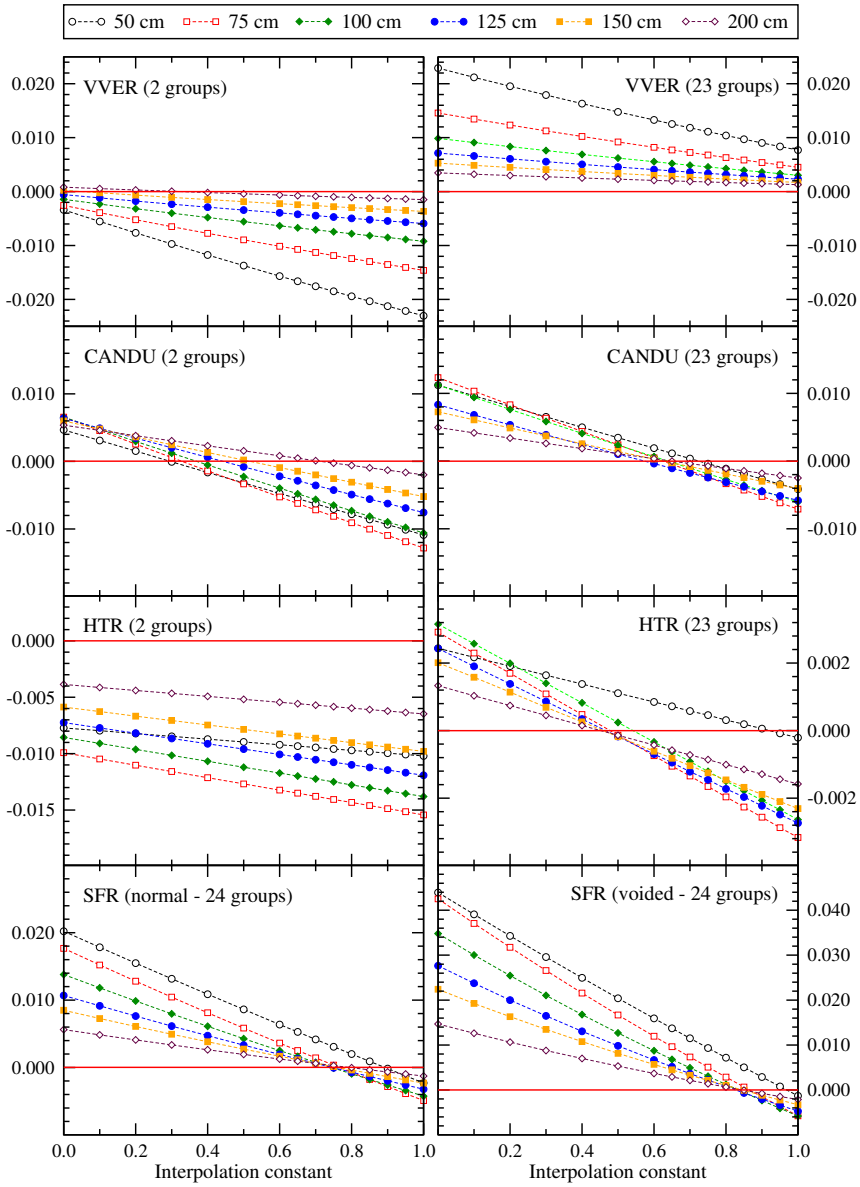

Figure 3.9. Differences in eigenvalues calculated by Monte Carlo (k_{MC}) and by diffusion theory (k_{dif}) for various simplified 1-D problems. XS data generated by Serpent for different system heights was fed to the TRIVAC code [12]. Diffusion calculations were performed using 50 axial meshes. Ordinate values correspond to $\Delta_k = (k_{MC} - k_{dif})$. The legend at the top indicates the height of the system. From Publication V.

Table 3.7. Optimal interpolation constants determined for the scenarios of Fig. 3.9. VVER and two-group HTR results do not yield equivalence and thus a confidence interval was not determined.

Cell type	m_{opt}	95 % confidence limits
VVER (2 groups)	0.00	n/a
VVER (23 groups)	1.00	n/a
CANDU (2 groups)	0.39	(0.14 – 0.64)
CANDU (23 groups)	0.64	(0.60 – 0.67)
HTR (2 groups)	0.00	n/a
HTR (23 groups)	0.48	(0.38 – 0.58)
SFR (normal)	0.76	(0.71 – 0.82)
SFR (voided)	0.84	(0.80 – 0.88)

is considerable. In HTR cells, an optimal value can only be determined for a sufficiently refined energy grid. SFR results are compatible with previous findings from Publication II, where more refined models yielded an optimal value $m = 0.85$.

3.4.1 Application to a CANDU reactor

A half-core CANDU benchmark problem was selected in order to test the performance of anisotropic diffusion coefficients taking into account the optimal interpolation constants of Table 3.7. The proposal by Pounders et al. [130] was simplified by modeling a fresh fuel core and by not including the reactivity control devices. Material temperature definitions were taken from another work [131].

Studies were conducted in two energy groups and also with an 8-group structure proposed by Pounders et al. [132]. Based on the results of Table 3.7, the interpolation constants $m = 0.40$ and $m = 0.65$ were used in conjunction with the 2- and 8-group structures, respectively.

In Publication V, this simplified benchmark problem was solved exploiting a variety of neutron leakage models at assembly level. The leakage model part of the study will be dealt with in Section 4.4 of the next chapter. Here, only the use of albedo boundary conditions at assembly level is dealt with.

The comparison of diffusion calculations and Monte Carlo reference values is summarized in Table 3.8. The agreement in 2-group eigenvalues is very poor, particularly in the case of directional diffusion coefficients, where the interpolation constant had been specifically adjusted to yield equivalence. Such adjustment, however, was conducted on 1-D systems along the

axial direction. In fact, Table 3.8 does report an improvement in the axial power comparison. It follows that the treatment of the radial component is troublesome.

Table 3.8. Results summary for CANDU problem using albedo boundary conditions during the XS generation process. The eigenvalue calculated with the code Serpent is $k\text{-}eff = 1.09585 \pm 0.00001$.

Energy bins	Model for D	$k\text{-}eff$	Δ_ρ (pcm)	$\Delta^{max}_{Pow}\|_{1D}$ (%)	$\Delta^{max}_{Pow}\|_{2D}$ (%)	$\Delta^{max}_{Pow}\|_{3D}$ (%)
2	Standard	1.09265	-267	0.92	1.57	2.31
	Anisotropic	1.09255	-276	0.82	3.07	3.19
8	Standard	1.09597	-10	0.50	1.39	1.48
	Anisotropic	1.09573	-10	0.41	2.49	2.57

$\Delta^{max}_{Pow}|_{1D}$: maximum relative difference in axial powers (12 axial regions).
$\Delta^{max}_{Pow}|_{2D}$: maximum relative difference in radial channel powers.
$\Delta^{max}_{Pow}|_{3D}$: maximum relative difference in fuel bundle powers.

Inspection of Fig. 3.4 b) reveals that some of the Cartesian mesh elements only intersect the moderator material, and thus the type of directional averaging method proposed fails to capture the nature of neutron diffusion in the homogenized system when heterogeneities are not uniformly distributed. In the SFR studies on hexagonal geometry (Publications II and III), such drawback was not experienced.

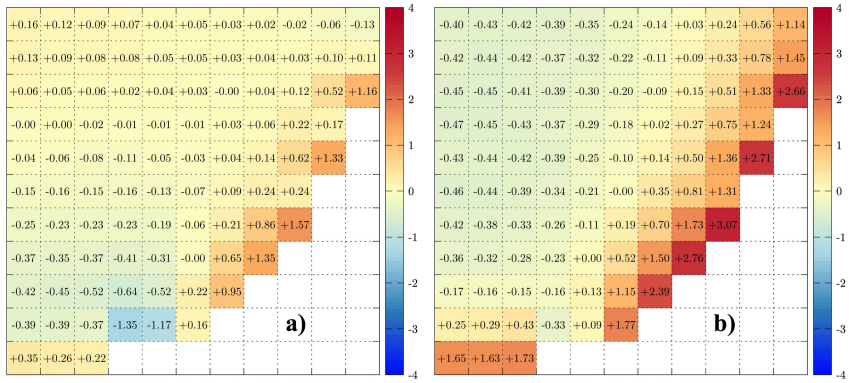

Figure 3.10. Radial power comparison for CANDU problem diffusion calculations performed in 2 energy groups using standard (a) and directional (b) diffusion coefficients. At every channel position, the legend denotes the relative difference between Monte Carlo and diffusion results, in percent. Adapted from Publication V.

8-energy-group results evidence a remarkable improvement in $k\text{-}eff$ for both diffusion coefficient models, which points out to the fact that the radial averaging problem is magnified when using 2 energy groups. To some

extent, however, the radial issue remains, because in Table 3.8 the performance of standard diffusion coefficients is still superior in terms of channel and bundle powers. In Fig. 3.10 b), the use of anisotropic diffusion coefficients induces a slight radial tilt in channel powers.

The quality of directional diffusion coefficients might be improved via a non-regular Cartesian mesh during cross section generation, in addition to a dedicated interpolation constant for the radial direction. However, the performance of standard diffusion coefficients is very satisfactory. Hence, improvements to the directional formalism are not easily justifiable.

3.5 Limitations

3.5.1 Micro-group structure

In the SFR studies, directional diffusion coefficients systematically yielded better results than isotropic diffusion coefficients. In Publication III, however, a study demonstrated that diffusion coefficients are susceptible to an undesirable dependence on the micro-group energy structure used in Serpent. The micro-group structure is used in an intermediate array where partial quantities are stored during the transport cycle, and then mapped onto the few-group array.

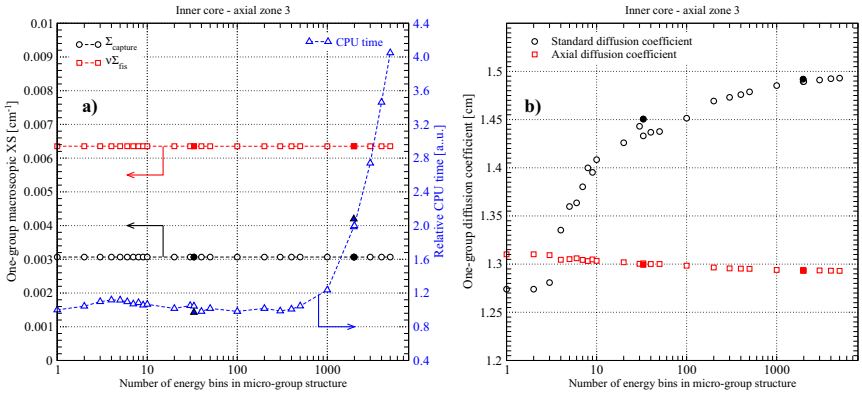

Figure 3.11. Selected one-group reaction XS data and relative computation time (a), and one-group diffusion coefficients (b) as a function of the number of energy bins in a uniform-lethargy micro-group structure ranging from 10^{-11} MeV to 20 MeV. Fully colored dots correspond to the non-uniform-lethargy structures ECCO-33 and ECCO-1968 [122]. Adapted from Publication III.

In Fig. 3.11, whereas the choice of the micro-group structure has an impact on the computing time, it has no effect on one-group reaction cross sec-

tion data. Conversely, standard and directional diffusion coefficients do show a dependence on the micro-group structure. This variation is associated with the summation of reciprocals in Eq. (2.16) and also when Eq. (2.24) is mapped from the micro- to the few-group array. The effect is more severe on standard diffusion coefficients. In multi-group problems, fine-structure effects are expected to be less prominent in the diffusion coefficients. The present studies, however, have not been focused on this matter.

Also in Publication III, discontinuity factors did improve the results, although the lack of leakage-corrected DFs in the radial direction and in some non-multiplicative regions limited the quality of the improvements.

The radial averaging techniques for directional diffusion coefficients proposed in Publication III are not fit for the treatment of cluster geometries typical in CANDU reactors, as arises from Publication V. This issue mainly affects the eigenvalue in two-group diffusion theory, although radial powers are also influenced for 2- as well as for 8-group structures.

3.5.2 On statistics in Publication I

In Publication I, Milgram's method was applied to simplified problems, with a view to allow tailoring the cross section data to suit the needs of that work. However, it would have been desirable to increase the computation time in order to improve the statistics of the results of Section 3.1. When that work was conducted, the premise was to characterize a qualitative functional dependence, and to underline the large uncertainties associated with Milgram's method when alternative techniques had already furnished well converged values.

4. Neutron leakage models in Monte Carlo XS generation

The first stage of the 2-step approach involves a solution of the neutron transport problem at lattice level. The means of capturing the physics of an infinite lattice is by the use of reflective or periodic boundary conditions.

The boundary conditions imposed at assembly level are generally not satisfied at core level. Hence, the performance of the homogenized few-group cross section data can be deteriorated due to the inability to capture neutron leakage in the first computational step. Because of this, corrections of the XS data at assembly level are mandatory. The problem is aggravated by the fact that the choice of the few-group structure may have a detrimental effect on the diffusion calculations or, conversely, result in some extent of error compensation that overrides the effect of the corrections.

Whereas the best means of representing assembly leakage is by explicitly modeling the –heterogeneous– surroundings, this approach can become computationally expensive. Furthermore, in a way this attempts against the idea of the two-step approach in the limit of large surroundings, since the full, heterogeneous core problem would be solved at the assembly level. A good leakage model is a trade-off between the improvement in the performance of the few-group XS data at core level and the complexity of the neutron transport problem solved at assembly level.

The focal point of this chapter is the comparison of various options to account for neutron leakage with the Monte Carlo code `Serpent 2`, and to compare the performance of such alternatives when applied to diffusion calculations. This chapter includes selected excerpts from Publications II–V.

4.1 On the explicit representation of surrounding assemblies: application to a fast reactor

It is expected that the effect of neutron leakage models is more pronounced in calculations involving only a reduced number of energy groups, since in such cases the real –continuous– neutron energy spectrum can undergo larger within-group variations, which affect the resulting few-group XS data.

In Publication II, the influence of the leakage model on the quality of full-core diffusion calculations of the ABR design in 7 energy groups was studied. Neutron leakage was accounted for via axially heterogeneous (or Z-heterogeneous) models, as well as by single fuel assemblies, followed by B_1 corrections[1] The energy structures used in Publication II are presented in Table 4.1.

Table 4.1. Energy group structures used in Publication II. Only upper bounds are reported. The lowest energy bound is 10^{-11} MeV.

24 g	7 g	Energy (MeV)	24 g	7 g	Energy (MeV)	24 g	7 g	Energy (MeV)
1	1	1.9640E+01	9		3.0197E-01	17	5	5.5308E-03
2		1.0000E+01	10		1.8316E-01	18		3.3546E-03
3		6.0653E+00	11	4	1.1109E-01	19	6	2.0347E-03
4	2	3.6788E+00	12		6.7379E-02	20		1.2341E-03
5		2.2313E+00	13		4.0868E-02	21		7.4852E-04
6	3	1.3534E+00	14		2.4788E-02	22		4.5400E-04
7		8.2085E-01	15		1.5034E-02	23		3.0432E-04
8		4.9787E-01	16		9.1188E-03	24	7	1.4863E-04

Regardless of the diffusion coefficient model, the results for normal and voided conditions of Table 4.2 and Table 4.3, respectively, indicate that Z-heterogeneous models have a better overall performance. Axially heterogeneous cross section generation models have the following advantages:

1. Improved fidelity of the neutron spectra in presence of explicit heterogeneous neutron leakage in the axial direction.

2. There is no need to postulate any space-energy separability of the neutron flux, as occurs with the B_1 corrections.

[1] In the case of the non-multiplicative assemblies (such as reflectors and control rod channels), a fuel region had to be added to the model, and no B_1 corrections were applied. B_1 corrections did not apply to XS data from other non-multiplicative zones listed in Table 3.2, either.

Table 4.2. Summary of 3-D ABR results for normal conditions using 7 energy groups. Reference eigenvalue from Serpent: *k-eff* $= 1.03732 \pm 0.00001$. Radial diffusion coefficients were obtained through the use of Eq. (2.25).

Model for D	Leakage treatment	*k-eff*	$\Delta\rho$ (pcm)	$\Delta^{max}_{Pow}\|_Z$ (%)	$\Delta^{max}_{Pow}\|_R$ (%)
standard	B_1	1.04280	+507	2.22	0.90
	Z-heterogeneous	1.03677	-51	0.50	1.04
anisotropic	B_1	1.04267	+494	2.53	0.96
	Z-heterogeneous	1.03725	-6	1.32	1.02

$\Delta^{max}_{Pow}|_Z$: maximum relative difference in axial power distribution.

$\Delta^{max}_{Pow}|_R$: maximum relative difference in radial power distribution.

Table 4.3. Summary of 3-D ABR results for voided conditions using 7 energy groups. Reference eigenvalue from Serpent: *k-eff* $= 1.05620 \pm 0.00001$. Radial diffusion coefficients were obtained through the use of Eq. (2.25).

Model for D	Leakage treatment	*k-eff*	$\Delta\rho$ (pcm)	$\Delta^{max}_{Pow}\|_Z$ (%)	$\Delta^{max}_{Pow}\|_R$ (%)
standard	B_1	1.06304	+609	2.40	0.93
	Z-heterogeneous	1.05948	+293	1.11	0.82
anisotropic	B_1	1.06229	+543	2.11	1.06
	Z-heterogeneous	1.05954	+298	1.45	0.78

$\Delta^{max}_{Pow}|_Z$: maximum relative difference in axial power distribution.

$\Delta^{max}_{Pow}|_R$: maximum relative difference in radial power distribution.

3. Monte Carlo codes such as `Serpent` are specially well suited for this type of three-dimensional setups.

4. XS data sets for several regions are generated simultaneously in a single run.

5. The availability of heterogeneous inter-region scalar fluxes and neutron currents can be exploited towards the generation of leakage-corrected discontinuity factors.

Z-heterogeneous models also suffer from some drawbacks:

1. Memory requirements are increased.

2. An adequate characterization of the surrounding environment and bound-

ary conditions is needed.

3. The number of neutron histories to be run is dictated by the region with the poorest statistics.

By adopting a coarse few-group structure, the spectral effect associated with the voiding of sodium from the ABR core cannot be properly captured, as emerges from the reactivity differences in Table 4.3. Also in Publication II, the number of energy groups was increased to 24. The results were already presented in Chapter 3, in the form of Table 3.3. The values reported therein suggest that there was a compensation of errors in the 7-group results for normal conditions. Leakage models cannot fully compensate the effect of a poor energy resolution.

In the context of Monte Carlo XS generation, the statistical precision of the few group data is directly linked to the CPU time, as discussed in connection with Eq. (2.15). By increasing the number of energy groups, one inevitably incurs in a computing time penalty, provided that the same degree of statistical precision is attained.

Increased CPU times are not associated with energy grid refinement only. In Publication III, axially heterogeneous models were applied to the generation of leakage-corrected discontinuity factors in the axial direction. As presented in Table 3.5, the quality of the results was improved, but the periodic radial boundary conditions imposed limited the extent of the enhancements. An attempt to extend the generation of leakage-corrected discontinuity factors to the radial direction through the explicit representation of neighboring assemblies plus vacuum boundary conditions would entail a combined memory and CPU computational burden that would render this approach impractical.

4.2 Generation of 3-D leakage-corrected discontinuity factors

The results of the preceding section bring to light that a detailed environment is beneficial in terms of the quality of the few-group XS data, although it can be at the same time detrimental from the point of view of CPU and memory requirements. For the sake of computational efficiency, it is of interest to model smaller systems, and use an adequate neutron leakage model.

In the particular case of leakage-corrected discontinuity factors, the need for non-zero net neutron currents at assembly boundaries rules out the use of

Table 4.4. Differences in reactivity between MC and diffusion calculations with albedo boundary conditions for different discontinuity factor models. Standard deviation in *k-eff* values computed by Serpent is 1 pcm. Standard diffusion coefficients were used in all cases. **UDF** cases use unity discontinuity factors. **DF**$_g$ cases use discontinuity factors from Generalized Equivalence Theory. **DF**$_l$ cases use leakage-corrected discontinuity factors.

k-eff	albedo	Δ_ρ (pcm)		
		UDF	DF$_g$	DF$_l$
1.16074	1.00000	3	3	3
1.15001	0.99914	-9	-7	-7
1.13751	0.99812	-10	-6	-5
1.12501	0.99708	-14	-7	-3
1.11251	0.99602	-15	-4	2
1.10001	0.99493	-22	-9	2

homogeneous B_1 theory. The results of Publication III show that it is possible to use the albedo heterogeneous leakage model available in `Serpent 2` in order to obtain leakage-corrected discontinuity factors. The performance of these DFs improves over that one of Generalized Equivalence Theory for a single node case, as presented in Table 4.4.

In Fig. 4.1, leakage-corrected discontinuity factors converge to those from Generalized Equivalence Theory in the limit of zero leakage.

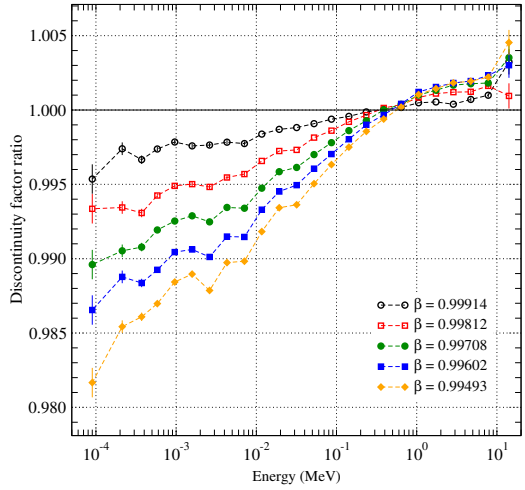

Figure 4.1. Radial leakage-corrected discontinuity factors (**DF**$_l$) normalized with discontinuity factors from Generalized Equivalence Theory (**DF**$_g$). The results are parametrized according to the albedo value (β). A table containing absolute values and their statistical uncertainties is included in Publication III.

4.3 Assembly-level comparison of neutron leakage methodologies

In Sections 4.1 and 4.2, the quality of some neutron leakage methodologies applied to diffusion calculations was assessed in a fast reactor system. In the interest of contrasting different leakage methods in a wider range of scenarios, it is convenient to isolate the cell calculation step from the core-level solution. In this way, neither the diffusion coefficient model nor the particular reactor setup will interfere with the comparisons.

In Publication IV, the following leakage methodologies:

- infinite medium (no spectral corrections),
- homogeneous B_1 corrections,
- albedo iterations, and
- layer-expansion-based leakage model

were applied to the study of a wide range of 2-D reactor cells. In addition to previous reactor designs, BWR and Pressurized Water Reactor (PWR), as well as plate-type, thermal-spectrum Materials Testing Reactor (MTR) fuel elements were added to the study. The MTR-CR case is a non-multiplicative, box-type MTR Control Rod, surrounded by MTR fuel.

The quality of every leakage option was judged based on the maximum relative differences in assembly-averaged multi-group scalar fluxes and pin powers. As a reference, a solution obtained by linear interpolation between two closest-to-critical colorsets was used.

A colorset is an extended cell, or super-cell of identical elements in a symmetrical arrangement. Typically, vacuum boundary conditions are applied, and few-group XS data constants are generated for the innermost element only. Additional considerations justifying the choice of colorset references are exposed in Section 4.5.1.

The full comparisons of assembly fluxes and pin powers of Table 4.5 and Table 4.6, respectively, have been summarized in the form of Table 4.7 in order to ease the analysis. The comparison is focused on the layer-expansion method[2] against infinite medium and albedo iterations only, for the sake of catering for the extreme scenarios where either no corrections at all, or detailed heterogeneous leakages were taken into account.

Referring to Table 4.7, the performance of the layer-expansion method is superior to the use of no corrections, whereas albedo search exhibits better

[2]Selected results correspond to the highest number of layers.

performance in reactor cells where neutrons travel large distances (CANDU, HTR and SFR). These maximum flux differences, however, occur in groups that do not contribute significantly to pin powers. In the case of the HTR cell, it should be born in mind that the maximum pin power difference with the layer-expansion method is within the bounds defined by the closest-to-critical colorsets, according to Table 4.6.

Table 4.5. Calculated maximum relative assembly flux differences (in percent) for various assembly leakage models. The maximum absolute uncertainty in the relative differences is $0.03\,\%$. Neutrons are always born in the central layer.

Cell type	Colorset		Single assembly					
	Lower	Upper	Infinite	B_1	Albedo	2 layers	3 layers	4 layers
BWR	0.19	0.85	3.09	1.43	4.12	3.77	1.77	–
CANDU	0.12	3.31	10.10	1.81	2.63	2.68	4.99	–
HTR	2.83	1.32	9.18	1.90	1.79	2.00	3.70	–
MTR	13.63	9.14	21.78	7.67	20.13	6.21	6.12	–
MTR-CR	16.89	7.65	8.95	–	3.89	2.11	–	–
PWR	2.94	2.77	6.20	1.78	7.09	3.97	3.91	–
SFR	1.94	4.37	22.59	3.21	12.90	13.63	22.42	21.58
VVER	17.64	2.41	13.66	2.71	12.42	10.89	6.32	–

Table 4.6. Calculated maximum relative pin power differences (in percent) for various assembly leakage models. The maximum absolute uncertainty in the relative differences is $0.01\,\%$, with the exception of infinite medium results for the SFR cell, where $0.06\,\%$ applies. Results corresponding to B_1 corrections were excluded, because they are the same as in the "Infinite" cases.

Cell type	Colorset		Single assembly				
	Lower	Upper	Infinite	Albedo	2 layers	3 layers	4 layers
BWR	0.09	0.39	1.20	1.80	1.92	1.64	–
CANDU	0.01	0.22	0.29	0.17	0.12	0.15	–
HTR	0.57	0.26	0.92	0.25	0.40	0.55	–
MTR	2.09	1.40	3.52	7.39	3.13	–	–
PWR	4.13	3.89	9.27	7.48	6.24	–	–
SFR	0.14	0.32	1.13	0.35	0.32	0.43	0.34
VVER	5.18	0.71	4.18	4.99	4.60	3.61	–

With regard to computational requirements, the layer-expansion method only incurs in a minor memory overhead, whereas the CPU time is either equivalent or slightly lower than in the case of albedo iterations, due to history termination by leakage. The results of Table 4.8 for BWR and PWR cells were obtained by running and averaging 250 cases per cell and per leakage model.

In multiplicative systems, the maximum number of layers determined by the algorithm of Fig. 2.3 a) will primarily depend on the difference between the infinite multiplication factor, k_∞, and the target eigenvalue, k_{target}. When

Table 4.7. Relative performance of the layer-expansion-based leakage model against infinite medium and albedo search methodologies. A tick mark (✓) indicates a better performance by the layer-expansion method. A dash sign (–) indicates that the values are comparable within their standard deviations. No powers were compared in the MTR control rod case.

Cell type	Fluxes		Powers	
	Infinite	Albedo	Infinite	Albedo
BWR	✓	✓	×	✓
CANDU	✓	×	✓	–
HTR	✓	×	✓	×
MTR	✓	✓	✓	✓
MTR-CR	✓	✓	n/a	n/a
PWR	✓	✓	✓	✓
SFR	✓	×	✓	–
VVER	✓	✓	✓	✓

Table 4.8. Averaged wall-clock computer time and memory overheads for heterogeneous leakage models. CPU times correspond to cases run using 12 tasks in Six-Core AMD Opteron 2435 2.6 GHz processors. Adapted from Publication IV.

Cell type	Leakage model	Time (min)	Memory (MB)
BWR	Albedo iterations	31.5 ± 0.2	377.32
	Layer expansion	32.0 ± 0.4	377.79
PWR	Albedo iterations	24.4 ± 0.1	874.85
	Layer expansion	23.4 ± 0.1	876.05

the excess reactivity is large, a low number of layers will suffice. As the difference decreases, or becomes negative[3], more layers will be necessary. Even in this situation, the layer-expansion algorithm will not incur in considerable computational overheads for two reasons:

1. The maximum number of layers needed is naturally limited by the neutron migration length, since neutrons are always born in the central position, as far away from the outer layer as possible. This results in system sizes smaller than the closest-to-critical colorsets. Moreover, the user can limit the maximum number of layers by input. The main CPU overheads envisaged are associated with the algorithms of Fig. 2.3 during the inactive cycles, and with weight modifications at some boundary crossings during

[3]In the case of $k_{target} > k_{\infty}$, the algorithm will resort to clustering, and an iteration value larger than unity will be enforced.

the active cycles. These costs should be comparable to those of the albedo iterations.

2. One of the main advantages of the trajectory expansion is that it relies on three integer indexes in order to identify any 3-D lattice element in the expanded system. There is no need to store additional assemblies in computer memory, irrespective of the number of layers. Consequently, the memory footprint of the method is very modest, and is mostly driven by the arrays used to tally layer-dependent fluxes. The user can also request 2-D multi-group flux maps (see Section 4.3.1), but this is an optional feature that can be overridden by input.

In scenarios where the assembly under study is sub-critical, either as a result of high burnup, boron concentration, or inserted control rods, the layer-expansion method will be susceptible to an increased variance of the iteration value due to a large number of layers, as will be discussed in Section 4.5.2.

No leakage model is able to account for what is not explicitly represented. Highly sub-critical (or non-multiplicative) assemblies will see their spectra more and more influenced by the neutron exchange with its neighbors as k_∞ decreases. In such situations, it is recommended to extend the XS model to include first neighbors. Even in these macro-cell environments, the layer-expansion method can be successfully applied, as demonstrated in the MTR-CR case in Table 4.5.

4.3.1 Layer-dependent fluxes

The unique index-based trajectory reconstruction feature exploited by the layer-expansion model can decouple the spatial and spectral components of the scalar neutron flux in a regular lattice by tallying layer-dependent spectra due to the neutrons originated in a single –central– lattice position. Examples of these special tallies are presented in Fig. 4.2.

Letting weight modifications aside, layer-dependent scalar fluxes satisfy reciprocity relations. For a single assembly with periodic or reflective boundary conditions, the scalar flux in such "central" element will be the direct sum of the contributions arising from all layers (in principle, the number of layers is unbound). If this system is now replaced by an equivalent infinite regular lattice of identical cells, and further assuming that a particular assembly embedded such lattice can be individualized, only the fluxes in the first layer of this assembly are due to neutrons born within such "central"

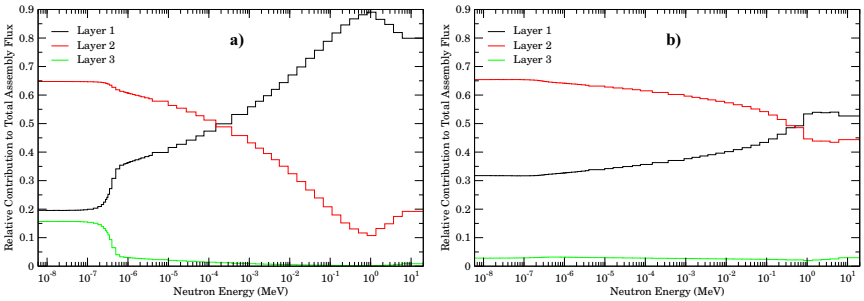

Figure 4.2. Layer-dependent scalar fluxes for CANDU (a) and VVER (b) assemblies. Neutrons are born in the central layer only. Adapted from Publication V.

position. This follows from the definition of the first layer.

All the remaining layer fluxes are due to neutrons that were born in other assemblies, and reached the central one. For those peripheral positions, reciprocally, the central assembly is located in some layer other than the first. Consequently, whilst the energy spectrum of neutrons dwelling in the first layer is a footprint of the central assembly, all higher layer fluxes are influenced by the neighbors.

In the CANDU case of Fig. 4.2 a), the fast flux is predominantly confined to layer 1. This means that most of the fast neutrons are born in the same central assembly, and only a reduced fraction of them reaches the neighboring surroundings. Conversely, thermal flux is predominant in layer 2, which implies that the majority of the thermal flux a CANDU assembly "sees" is actually due to neutrons born in first-neighbor assemblies. These distinctive behaviors are due to the combined effect of cluster geometry and large migration lengths, and are more tangible in the two-group results of Fig. 4.3.

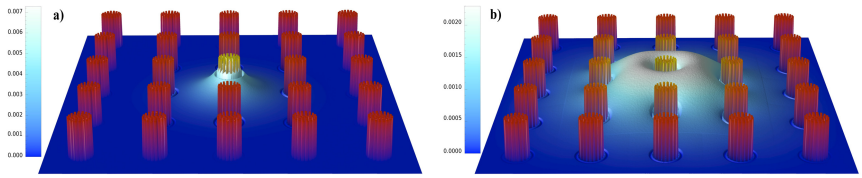

Figure 4.3. Fast (a) and thermal (b) expanded scalar fluxes in a fresh CANDU cell. Fluxes due to neutrons born only in the central lattice element are tallied at collision sites. In fissile regions, colors ranging from red to yellow depict the fission rate, in arbitrary units. Adapted from Publication V.

In the VVER case of Fig. 4.2 b), the spectral variations per layer are not so pronounced, which suggests that for this type of cells the environment of a given assembly has less effect on the spectrum "seen" by that element.

The layer-expansion technique provides valuable insights on the space-

energy properties of the scalar flux in a regular lattice, and can be helpful in understanding what are the characteristic length scales that neutronically couple different fuel elements in a reactor core.

4.4 Leakage models applied to a CANDU reactor

In Publication V, different strategies were applied in order to account for neutron leakage during few-group XS generation with `Serpent 2`. Since it is expected that group collapsing effects are more severe in coarse energy grids, cross section generation and diffusion calculations were carried out in 2 and in 8 energy groups. The latter energy structure definition may be found in Publication V. The results are presented in Table 4.9.

Table 4.9. Results summary for simplified CANDU benchmark problem using standard diffusion coefficients. No leakage corrections were applied in the reflector region in the B_1 cases. Serpent eigenvalue: *k-eff* $= 1.09587 \pm 0.00001$. Relative uncertainties in maximum channel (0.02%) and bundle (0.09%) power differences are governed by the quality of the MC solution. Adapted from Publication V.

Energy bins	Leakage model	*k-eff*	Δ_ρ (pcm)	$\Delta^{max}_{Pow}\|_{1D}$ (%)	$\Delta^{max}_{Pow}\|_{2D}$ (%)	$\Delta^{max}_{Pow}\|_{3D}$ (%)
2	Infinite lattice	1.09289	-247	0.91	1.73	2.67
	B_1	1.09149	-365	0.89	2.15	2.28
	Albedo	1.09265	-267	0.92	1.57	2.31
	Layer expansion	1.09270	-263	0.92	1.60	2.56
8	Infinite lattice	1.09631	+38	0.50	1.31	1.51
	B_1	1.09537	-40	0.48	1.79	1.88
	Albedo	1.09597	+10	0.50	1.39	1.48
	Layer expansion	1.09632	+39	0.50	1.22	1.61

$\Delta^{max}_{Pow}|_{1D}$: maximum relative difference in axial powers (12 axial regions).

$\Delta^{max}_{Pow}|_{2D}$: maximum relative difference in radial channel powers.

$\Delta^{max}_{Pow}|_{3D}$: maximum relative difference in fuel bundle powers.

The effect of energy collapsing is readily noticeable in the 2-group results. The differences in reactivity are in agreement with results by Shen [133]. In the case of B_1 corrections, the agreement in eigenvalue is particularly deteriorated. Heterogeneous leakage models (albedo, layer expansion) yield better results, which differ only slightly among them.

The overall agreement in eigenvalue and power distribution is remarkably improved when a finer, 8-group structure is used. This exercise confirms that leakage models cannot entirely correct combined homogenization and condensation errors. In the framework of the two-step core analysis approach with a coarse energy mesh, it is recommended that leakage-corrected

discontinuity factors are generated as a means of reducing these errors. It is pertinent to point out that, from the methods listed in Table 4.9, only the albedo and layer-expansion schemes can provide the face-averaged net currents required for this task.

In Publication V, a CANDU benchmark problem was adopted mostly due to directional diffusion coefficient considerations, and was not necessarily the best motif for a conclusive evaluation of leakage models beyond the observations of the preceding paragraphs. It is not possible to assert, at this stage, that the similar performance of albedo and layer-expansion methods will hold in other reactor types. Further studies focused on other systems are envisaged as future work.

4.5 Limitations

4.5.1 About the reference solution

In Publication IV, a linear interpolation technique between values obtained from the two closest-to-critical colorsets was adopted as a source of reference data for comparison. Denoting the "lower" (i.e., sub-critical) colorset by the superscript "l", and by the superscript "u" the "upper" (super-critical) colorset, any reference quantity χ^r was computed by linear interpolation of the corresponding colorset quantities $\left(\chi^l, \chi^u\right)$ and their associated eigenvalues, $\left(k^l, k^u\right)$, through:

$$\chi^r = \frac{k^u - 1}{k^u - k^l}\,\chi^l + \frac{1 - k^l}{k^u - k^l}\,\chi^u\,. \tag{4.1}$$

In Eq. (4.1), the quantity χ may be a multi-group flux, a pin power, or a face-averaged multi-group albedo. The use of interpolation was driven by the need to reduce two discrete data sets into a single one. In addition to Table 4.5 and Table 4.6, calculated multi-group albedos depicted in Fig. 4.4 also highlight the extent of variability that can be expected between closest-to-critical colorsets.

The assumption of linear behavior is undoubtedly conjectural, but given the discrete nature of the bounding colorsets, the procurement of any intermediate solution will entail some extent of approximation.

It is fair to question the choice of colorsets as sources of reference values altogether, knowing that more reliable figures would originate from heterogeneous, full-core systems. Had the latter approach been opted for, then the computational requirements would have increased dramatically.

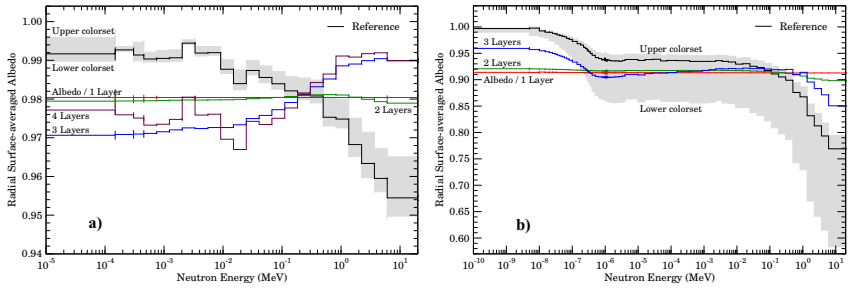

Figure 4.4. Calculated radial albedos for SFR (a) and VVER (b) cases. The gray area highlights the extent of variability that can be expected depending on the size of the colorset used. Adapted from Publication IV.

At the expense of much extra work, the calculation burden could have been alleviated via global-local iterations, with embedded Monte Carlo cell calculations constrained by boundary neutron currents provided by a core-level diffusion solver. The results of Cho et al. [118], however, evidence slow convergence and an apparent bias in this approach.

In the work by Leppänen et al. [90], large colorsets were shown to provide the best characterization of assembly environments in a highly heterogeneous core fueled with uranium dioxide (UO_2), and including burnable absorber pins and control rods. The performance of those colorsets was also taken into account during the choice of the reference scenarios in Publication IV.

4.5.2 Layer-expansion leakage model: sensitivity study

Neutron weight updates in the layer-expansion-based leakage model do not occur, in the general case, at every lattice surface crossing, as happens in the case of albedo iterations. The relatively infrequent nature of the weight modifications is manifested in the statistical spread of the system eigenvalues obtained by layer expansion.

In Publication IV, a sensitivity study for PWR and BWR cells was conducted by running several identical cases with different random seeds, in order to guarantee statistical independence. The results are presented in the form of histograms in Fig. 4.5.

The dispersion of the eigenvalues associated with the layer-expansion method can be reduced by increasing the number of inactive cycles, at the expense of increased computation time. It is expected, nonetheless, that cells with eigenvalues that depart a few hundred pcm from their target values will still yield better leakage-corrected spectra than in the infinite lattice

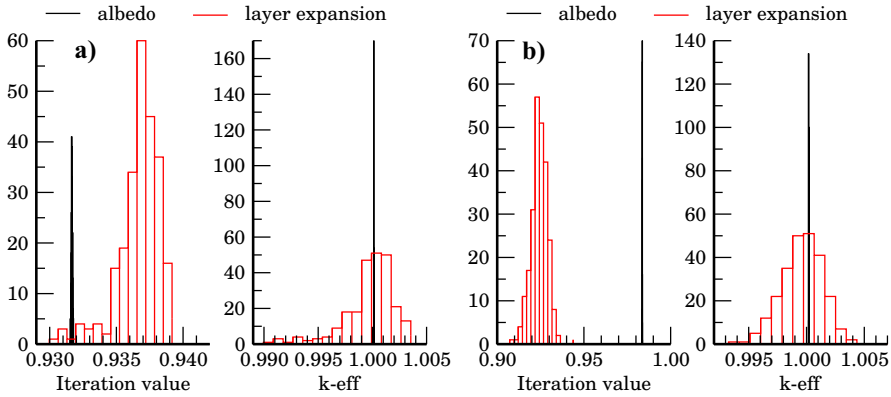

Figure 4.5. Statistical distribution of iteration value and eigenvalue for PWR (a) and BWR (b) cells. For comparison purposes, the results obtained via albedo criticality search are also included. Every data set was obtained by post-processing the results of 250 independent Monte Carlo calculations. Adapted from Publication IV.

model without any corrections.

5. Conclusions

5.1 Implications

The adoption of different Monte Carlo techniques for the computation of multi-group diffusion coefficients may have a considerable effect on the agreement between full-core diffusion results and reference values procured by a detailed Monte Carlo transport simulation. In SFR applications, the newly introduced anisotropic diffusion coefficient formalism performed remarkably better than the use of previous –isotropic– diffusion coefficients with unity discontinuity factors.

The treatment of control rods was challenging for both diffusion coefficient models. The root cause of this is not intrinsic to the diffusion coefficients, but to the validity of the diffusion approximation altogether. Whereas discontinuity factors improved the quality of the solutions, the improvements were lessened due to the lack of leakage-corrected radial DFs, as well as to the emergence of negative homogeneous fluxes in some non-multiplicative regions. In situations like these, anisotropic diffusion coefficients are more convenient. The introduction of internal boundary conditions, a relatively simple technique, was more successful in the evaluation of control rod worth, which is an extremely important safety parameter.

The need for improvements in the calculation methods for control rods in fast reactors was already identified, for example, by Gauthier et al. [134]. The advantages of the IBC implementation described in this work are that: IBCs were readily available from data required for the calculation of discontinuity factors; current-to-flux ratios required only minor modifications to the diffusion solver; and no post-processing of the diffusion results was necessary.

In order to improve the performance of diffusion coefficients under voided

conditions, leakage corrections are necessary also in the radial direction. To that end, the heterogeneous leakage models at assembly level studied in this thesis can provide the net neutron currents required for this task. This reinforces the introductory claim (see Section 1.2) that diffusion coefficients and leakage models are coupled.

Homogeneous B_1 corrections in SFR and CANDU cases yielded the worst overall agreement against transport results. In consequence, either albedo or layer-expansion methods are recommended. It is also important to remark that refining the energy grid had a more beneficial effect than the choice of the leakage model. If computational speed constraints force the adoption of a coarse energy structure, the energy condensation error can be compensated by generating leakage-corrected discontinuity factors with the help of heterogeneous leakage models.

The CANDU scenario was not optimal for an exhaustive comparison between albedo and layer-expansion leakage models. In spite of this, the concept of layer expansion furnishes valuable information about the space-energy coupling of the scalar neutron flux in any type of reactor assembly embedded in a lattice.

5.2 Limitations of the research

The numerical methods implemented in `Serpent 2` and all the related code modifications have not been optimized, and were developed for the sake of this research only. None of these changes constitutes a part of the software package.

The main findings of this research are limited to the reactor systems considered. A study on the generalization of anisotropic diffusion coefficients to diverse reactor types provided some insights, including their inapplicability to light water reactors[1]. The same study, however, suggested that CANDU reactors were good candidates for the application of the formalism, until detailed 3-D calculations revealed deficiencies in the radial averaging technique for cluster geometry.

A more comprehensive study on the effect of the micro-group structure on the diffusion coefficients condensed over several groups is still missing.

The larger variances associated with the layer-expansion leakage model were not directly discernible in the results. As stated earlier, a reactor system other than CANDU would have been more suitable for the comparison

[1] At least, in the limit of very coarse and very fine energy grids.

between heterogeneous leakage models in the 2-step approach.

5.3 Recommendations for future research

The limitations raised in Section 5.2 provide motivation for future research. The application of the layer-expansion leakage model to different types of reactor cells may shed light on features that were not accessible through previous methods. Pertaining directional diffusion coefficients, preliminary results suggest that the application of the new methodology to graphite-moderated, gas-cooled reactors is worthwhile investigating.

Advanced leakage models may impact the quality of the depletion calculations used in source term analysis. This, in turn, may have implications that range from fuel performance to shielding analysis and fuel disposal. In the near future, the main beneficiaries of this research will be prospective students and other colleagues.

Bibliography

[1] J. Houghton, "Global warming," *Rep Prog Phys*, no. 68, pp. 1343–1403, 2005.

[2] G. McCracken and P. Stott, *Fusion – The Energy of the Universe*. Academic Press, 2nd ed., 2013.

[3] U.S. DOE Nuclear Energy Research Advisory Committee and the Generation IV International Forum, "A Technology Roadmap for Generation IV Nuclear Energy Systems," Tech. Rep. GIF-002-00, NERAC and GIF, December 2002.

[4] J. Rouault, P. Chellapandi, B. Raj, P. Dufour, C. Latge, L. Paret, P. L. Pinto, G. H. Rodriguez, G.-M. Gautier, G.-L. Fiorini, M. Pelletier, D. Gosset, S. Bourganel, G. Mignot, F. Varaine, B. Valentin, P. Masoni, P. Martin, J.-C. Queval, D. Broc, and N. Devictor, "Sodium Fast Reactor Design: Fuels, Neutronics, Thermal-Hydraulics, Structural Mechanics and Safety," in *Handbook of Nuclear Engineering* (D. G. Cacuci, ed.), vol. 4, ch. 21, pp. 2321–2710, Springer, 1st ed., 2010.

[5] G. Rimpault, D. Plisson, J. Tommasi, R. Jacqmin, J.-M. Rieuner, D. Verrier, and D. Biron, "The ERANOS code and data system for fast reactor neutronic analyses," in *ANS Reactor Physics Topical Meeting (PHYSOR 2002)*, (Seoul, Korea, October 7–10), 2002.

[6] K. Mikityuk, S. Pelloni, P. Coddington, E. Bubelis, and R. Chawla, "FAST: An advanced code system for fast reactor transient analysis," *Ann Nucl Energy*, vol. 32, pp. 1613–1631, 2005.

[7] E. Fridman, R. Rachamin, and E. Shwageraus, "Generation of SFR Few-Group Constants Using the Monte Carlo Code Serpent," in *International Conference on Mathematics and Computational Methods Applied to Nuclear Science and Engineering (M&C 2013)*, (Sun Valley, Idaho, USA, May 5–9), 2013.

[8] E. Nikitin, E. Fridman, and K. Mikityuk, "Solution of the OECD/NEA neutronic SFR benchmark with Serpent-DYN3D and Serpent-PARCS code systems," *Ann Nucl Energy*, vol. 75, pp. 492–497, 2015.

[9] J. Leppänen, M. Pusa, T. Viitanen, V. Valtavirta, and T. Kaltiaisenaho, "The Serpent Monte Carlo code: Status, development and applications in 2013," *Ann Nucl Energy*, vol. 82, pp. 142–150, 2015.

[10] A. Koning, R. Forrest, M. Kellett, R. Mills, H. Henriksson, and Y. R. (Eds.), "The JEFF-3.1 Nuclear Data Library," Tech. Rep. JEFF Report 21, Nuclear Energy Agency (NEA), 2006.

[11] E. Dorval, "TRIZ: Multi-Group Neutron Diffusion in Triangular-Z Geometry. Version 1.0," Tech. Rep. FF-2014-01, Aalto University School of Science, 2014.

[12] A. Hébert, "A user guide for TRIVAC Version4," Tech. Rep. IGE-293, École Polytechnique de Montréal, September 2012.

[13] A. K. Prinja and E. W. Larsen, "General Principles of Neutron Transport," in *Handbook of Nuclear Engineering* (D. G. Cacuci, ed.), vol. 2, ch. 5, pp. 427–542, Springer, 1st ed., 2010.

[14] W. M. Stacey, *Nuclear Reactor Physics*. John Wiley & Sons, 1st ed., 2001.

[15] E. E. Lewis and W. F. Miller, Jr, *Computational Methods of Neutron Transport*. John Wiley & Sons, 1st ed., 1984.

[16] C. R. E. de Oliveira and A. J. H. Goddard, "EVENT – A Multidimensional Finite Element-Spherical Harmonics Radiation Transport Code," in *Proceedings of the OECD International Seminar on 3D Deterministic Radiation Transport Codes*, (Paris), 1996.

[17] J. K. Fletcher, "A Users Guide to the MARC/PN Computer Code," Tech. Rep. TRG 291 1(R), United Kingdom Atomic Energy Authority, 1976.

[18] "WIMS, MultiGroup Reactor Lattice Calculation for Thermal Reactor and Fast Reactor." Software package NEA-0329 WIMS-D/4.

[19] E. Villarino, "CONDOR calculation package," in *ANS Reactor Physics Topical Meeting (PHYSOR 2002)*, (Seoul, Korea, October 7–10), 2002.

[20] M. D. DeHart, "NEWT: A New Transport Algorithm for Two-Dimensional Discrete Ordinates Analysis in Non-Orthogonal Geometries," Tech. Rep. ORNL/TM-2005/39 Vol. II Sect. F21, Oak Ridge National Laboratory, January 2009.

[21] N. M. Greene and L. M. Petrie, "XSDRNPM: A One-Dimensional Discrete-Ordinates Code for Transport Analysis," Tech. Rep. ORNL/TM-2005/39 Vol. II Sect. F3, Oak Ridge National Laboratory, January 2009.

[22] "CASMO-4 A Fuel Assembly Burnup Program," Tech. Rep. SSP-09/443-U Rev 0, Studsvik Scandpower, Inc., 2009.

[23] G. Marleau, A. Hébert, and R. Roy, "A User Guide for DRAGON version 000331 Release 3.04,," Tech. Rep. IGE-174. Rev 5, École Polytechnique de Montréal, September 2000.

[24] R. Sanchez, I. Zmijarevic, M. Coste-Delclaux, E. Masiello, S. Santandrea, E. Martinolli, L. Villate, N. Schwartz, and N. Gulers, "APOLLO2 Year 2010," *Nucl Eng Technol*, vol. 42, no. 5, pp. 474–499, 2010.

[25] C. Wemple, H. Gheorghiu, R. J. J. Stamm'ler, and E. Villarino, "Recent Advances in the HELIOS-2 Lattice Physics Code," in *ANS Reactor Physics Topical Meeting (PHYSOR 2008)*, (Interlaken, Switzerland, September 14–19), 2008.

[26] R. Sanchez and N. J. McCormick, "A Review of Neutron Transport Approximations," *Nucl Sci Eng*, vol. 80, pp. 451–535, 1982.

[27] R. Roy, "Reactor Core Methods," in *Nuclear Computational Science: A Century in Review* (Y. Azmy and E. Sartori, eds.), ch. 4, pp. 167–215, Springer, 1st ed., 2010.

[28] R. J. J. Stamm'ler and M. J. Abbate, *Methods of Steady-State Reactor Physics in Nuclear Design*. Academic Press, 1st ed., 1983.

[29] J. J. Duderstadt and L. J. Hamilton, *Nuclear Reactor Analysis*. John Wiley & Sons, 1st ed., 1976.

[30] A. Hébert, *Applied Reactor Physics*. Presses internationales Polytechnique, 1st ed., 2009.

[31] P. S. Brantley and E. W. Larsen, "The Simplified P_3 Approximation," *Nucl Sci Eng*, vol. 134, pp. 1–21, 2000.

[32] P. Kotiluoto, "Fast Tree Multigrid Transport Application for the Simplified P_3 Approximation," *Nucl Sci Eng*, vol. 138, pp. 269–278, 2001.

[33] S. Duerigen, U. Grundmann, S. Mittag, B. Merk, E. Fridman, and S. Kliem, "A Trigonal Nodal Solution Approach to the Multi-Group Simplified P_3 Equations in the Reactor Code DYN3D," in *International Conference on Mathematics and Computational Methods Applied to Nuclear Science and Engineering (M&C 2011)*, (Rio de Janeiro, RJ, Brazil, May 8–12), 2011.

[34] C. Sandrin, R. Sanchez, and F. Dolci, "An Analysis of Reflector Homogenization Techniques for Full Core Diffusion Calculations," *Nucl Sci Eng*, vol. 168, pp. 59–72, 2011.

[35] N. Z. Cho, "Fundamentals and Recent Developments of Reactor Physics Methods," *Nucl Eng Technol*, vol. 37, no. 1, pp. 25–78, 2005.

[36] P. Benoist, "Formulation générale et calcul pratique du coefficient de diffusion dans un réseau comportant des cavités," Tech. Rep. 1354, CEA – Centre d'Études Nucléaires de Saclay, 1959.

[37] P. Benoist, "A Simple Model for the Calculation of the Sodium-Voiding Effect on Neutron Leakages in a Fast Reactor Lattice I. Formalism," *Nucl Sci Eng*, vol. 86, pp. 22–40, 1984.

[38] T. Takeda and T. Sekiya, "Calculation of the Anisotropic Diffusion Coefficient," *J Nucl Sci Technol*, vol. 9, no. 12, pp. 697–704, 1972.

[39] O. J. Sheaks and L. H. Sulivan, "Multigroup Diffusion Coefficients from Transport Theory," *Nucl Sci Eng*, vol. 51, pp. 331–343, 1973.

[40] T. Yoshida and S. Iijima, "Numerical Study on Applicability of Benoist's Diffusion Coefficient to Sodium Void Reactivity Analysis," *J Nucl Sci Technol*, vol. 13, no. 8, pp. 464–467, 1976.

[41] J. L. Rowlands and C. R. Eaton, "Effective Diffusion Coefficients for Low Density Cylindrical Channels," *Nucl Sci Eng*, vol. 76, pp. 263–281, 1980.

[42] K. Kobayashi, "Efficient Method for Calculating Axial Diffusion Coefficients in Two-Dimensional Low Density Channel," *J Nucl Sci Technol*, vol. 28, no. 8, pp. 757–766, 1990.

[43] K. Azekura, "A Modified Diffusion Coefficient for Heterogeneous Low-Density Channels," *J Nucl Sci Technol*, vol. 32, no. 6, pp. 557–583, 1995.

[44] M. M. R. Williams, "Anisotropic diffusion coefficients and the streaming problem in slab lattices: A new approach," *Prog Nucl Energ*, vol. 71, pp. 89–116, 2014.

[45] J. M. Pounders and F. Rahnema, "On the Diffusion Coefficients for Reactor Physics Applications," *Nucl Sci Eng*, vol. 163, pp. 243–262, 2009.

[46] K. Koebke, "A New Approach to Homogenization and Group Condensation," Tech. Rep. IAEA-TECDOC-231, International Atomic Energy Agency, 1978.

[47] K. S. Smith, *Spatial Homogenization Methods for Light Water Reactor Analysis*. PhD thesis, Massachusetts Institute of Technology, 1980.

[48] K. S. Smith, "Assembly homogenization techniques for light water reactor analysis," *Prog Nucl Energy*, vol. 17, no. 3, pp. 303–335, 1986.

[49] T. M. Sutton and B. N. Aviles, "Diffusion Theory Methods for Spatial Kinetics Calculations," *Prog Nucl Energ*, vol. 30, no. 2, pp. 119–182, 1996.

[50] T. DeLorey, *A Transient, Quadratic Nodal Method for Triangular-Z Geometry*. PhD thesis, Massachusetts Institute of Technology, 1993.

[51] J. P. Roos, "Some numerical schemes for neutron diffusion problems," Tech. Rep. EUR 3262.e, European Atomic Energy Community (EURATOM), 1967.

[52] D. R. Ferguson and K. L. Derstine, "Optimized Iteration Strategies and Data Management Considerations for Fast Reactor Finite Difference Diffusion Theory Codes," *Nucl Sci Eng*, vol. 64, pp. 593–604, 1977.

[53] T. B. Fowler, D. R. Vondy, and G. W. Cunningham, "Nuclear Reactor Core Analysis Code CITATION," Tech. Rep. ORNL-TM-2496, Oak Ridge National Laboratory, 1971.

[54] K. L. Derstine, "DIF3D: A Code to Solve One-, Two-, and Three-Dimensional Finite-Difference Diffusion Theory Problems," Tech. Rep. ANL-82-64, Argonne National Laboratory, 1984.

[55] Y. Kato, T. Takeda, and S. Takeda, "A Coarse-Mesh Correction of the Finite Difference Method for Neutron Diffusion Calculations," *Nucl Sci Eng*, vol. 61, pp. 127–141, 1976.

[56] G. Buckel, K. Küfner, and B. Stehle, "Benchmark Calculations for a Sodium-Cooled Breeder Reactor by Two- and Three-Dimensional Diffusion Methods," *Nucl Sci Eng*, vol. 64, pp. 75–89, 1977.

[57] Computational Benchmark Problems Committee of the Mathematics and Computation Division of the American Nuclear Society, "Argonne Code Center: Benchmark Problem Book," Tech. Rep. ANL-7416, Supplement 2, Argonne National Laboratory, June 1977.

[58] L. F. Richardson, "The approximate arithmetical solution by finite differences of physical problems involving differential equations with an application to the stresses in a masonry dam," *Transactions of the Royal Society of London*, no. 210, pp. 307 – 357, 1910.

[59] L. F. Richardson and J. A. Gaunt, "The Deferred Approach to the Limit. Part I. Single Lattice. Part II. Interpenetrating Lattices," *Transactions of the Royal Society of London*, no. 226, pp. 299 – 361, 1927.

[60] R. D. Lawrence, "Progress in nodal methods for the solution of the neutron diffusion and transport equations," *Prog Nucl Energy*, vol. 17, no. 3, pp. 271–301, 1986.

[61] Y. A. Chao and N. Tsoulfanidis, "Conformal Mapping and Hexagonal Nodal Methods – I: Mathematical Foundation," *Nucl Sci Eng*, vol. 121, pp. 202–209, 1995.

[62] Y. A. Chao and Y. A. Shatilla, "Conformal Mapping and Hexagonal Nodal Methods – II: Implementation in the ANC-H Code," *Nucl Sci Eng*, vol. 121, pp. 210–225, 1995.

[63] N. Z. Cho and J. Lee, "Analytic Function Expansion Nodal (AFEN) Method in Hexagonal-Z Three-Dimensional Geometry for Neutron Diffusion Calculation," *J Nucl Sci Technol*, vol. 43, no. 11, pp. 1320–1326, 2006.

[64] J. Y. Cho and C. H. Kim, "Higher order polynomial expansion nodal method for hexagonal core neutronics analysis," *Ann Nucl Energy*, vol. 25, no. 13, pp. 1021–1031, 1998.

[65] T. Downar, D. Lee, Y. Xu, T. Kozlowski, and J. Staudenmier, "PARCS v2.6 U.S. NRC Core Neutronics Simulator USER MANUAL Draft (11/10/04)," tech. rep., Purdue University and U.S. NRC, 2004.

[66] R. Mattila, "Three-Dimensional Analytic Function Expansion Nodal Model," Tech. Rep. YEPD-9/2002, VTT Technical Research Centre of Finland, 2002.

[67] U. Grundmann, U. Rohde, and S. Mittag, "DYN3D – three-dimensional core model for steady-state and transient analysis of thermal reactors," in *ANS Reactor Physics Topical Meeting (PHYSOR 2000)*, (Pittsburgh, Pennsylvania, USA, May 7–11), 2000.

[68] N. Metropolis and S. Ulam, "The Monte Carlo Method," *J Am Stat Assoc*, vol. 44, no. 247, pp. 335–341, 1949.

[69] N. Metropolis, "The Beginning of The Monte Carlo Method," *Los Alamos Science*, vol. 15, pp. 125–130, 1987.

[70] J. Spanier and E. M. Gelbard, *Monte Carlo Principles and Neutron Transport Problems*. Dover Publications, Inc., 1st ed., 2008.

[71] X-5 Monte Carlo Team, "MCNP – A General Monte Carlo N-Particle Transport Code, Version 5," Tech. Rep. LA-UR-03-1987, vol. I: Overview and Theory, Los Alamos National Laboratory, 2003 (Revised 2008).

[72] C. M. Diop, O. Petit, E. Dumonteil, F. X. Hugot, Y. K. Lee, A. Mazzolo, and J. C. Trama, "TRIPOLI-4: a 3D continuous-energy Monte Carlo transport code," in *PHYTRA1: First International Conference on Physics and Technology of Reactors and Applications*, (Marrakech, Morocco, March 14–16), 2007.

[73] R. N. Blomquist, R. M. Lell, and E. M. Gelbard, "VIM – A Continuous Energy Monte Carlo Code at ANL," Tech. Rep. ORNL/RSIC-44, 1980.

[74] P. Cowan, G. Dobson, and J. Martin, "Release of MCBEND 11," *Prog Nucl Sci Technol*, vol. 4, pp. 437–440, 2014.

[75] S. P. Pederson, R. A. Forster, and T. E. Booth, "Confidence Interval Procedures for Monte Carlo Transport Simulations," *Nucl Sci Eng*, vol. 127, pp. 54–77, 1997.

[76] F. B. Brown, "A Review of Monte Carlo Criticality Calculations – Convergence, Bias, Statistics," Tech. Rep. LA-UR-08-06558, Los Alamos National Laboratory, 2008.

[77] W. R. Martin, "Challenges and Prospects for Whole-Core Monte Carlo Analysis," *Nucl Eng Technol*, vol. 44, no. 2, pp. 151–160, 2012.

[78] B. T. Mervin, S. W. Mosher, J. C. Wagner, and G. I. Maldonado, "Uncertainty Underprediction in Monte Carlo Eigenvalue Calculations," *Nucl Sci Eng*, vol. 173, pp. 276–292, 2013.

[79] P. K. Romano and B. Forget, "The OpenMC Monte Carlo particle transport code," *Ann Nucl Energy*, vol. 51, pp. 274–281, 2013.

[80] K. Wang, Z. Li, D. She, Y. Liu, Q. Xu, H. Shen, and G. Yu, "Progress on RMC – A Monte Carlo neutron transport code for reactor analysis," in *International Conference on Mathematics and Computational Methods Applied to Nuclear Science and Engineering (M&C 2011)*, (Rio de Janeiro, RJ, Brazil, May 8–12), 2011.

[81] H. J. Park, H. J. Shim, H. G. Joo, and C. H. Kim, "Generation of Few-Group Diffusion Theory Constants by Monte Carlo Code McCARD," *Nucl Sci Eng*, vol. 172, pp. 66–77, 2012.

[82] J. Leppänen, *Development of a New Monte Carlo Reactor Physics Code*. PhD thesis, Helsinki University of Technology, 2007.

[83] "OECD/NEA Data Bank Computer Program Services." https://www.oecd-nea.org/dbprog/. Accessed: 2015-12-29.

[84] " Radiation Safety Information Computational Center." https://rsicc.ornl.gov/. Accessed: 2015-12-29.

[85] J. Leppänen, "Performance of Woodcock delta-tracking in lattice physics applications using the Serpent Monte Carlo reactor physics burnup calculation code," *Ann Nucl Energy*, vol. 37, pp. 715–722, 2010.

[86] J. Leppänen, "Two practical methods for unionized energy grid construction in continuous-energy Monte Carlo neutron transport calculation," *Ann Nucl Energy*, vol. 36, pp. 878–885, 2009.

[87] "Serpent – A Continuous-energy Monte Carlo Reactor Physics Burnup Calculation Code." http://montecarlo.vtt.fi. Accessed: 2015-11-16.

[88] E. Fridman and J. Leppänen, "On the use of the Serpent Monte Carlo code for few-group cross section generation," *Ann Nucl Energy*, vol. 38, pp. 1399–1405, 2011.

[89] E. Fridman and E. Shwageraus, "Modeling of SFR cores with Serpent-DYN3D codes sequence," *Ann Nucl Energy*, vol. 53, pp. 354–363, 2013.

[90] J. Leppänen, R. Mattila, and M. Pusa, "Validation of the Serpent-ARES code sequence using the MIT BEAVRS benchmark – Initial core at HZP conditions," *Ann Nucl Energy*, vol. 69, pp. 212–225, 2014.

[91] R. Rachamin, C. Wemple, and E. Fridman, "Neutronic analysis of SFR core with HELIOS-2, Serpent, and DYN3D codes," *Ann Nucl Energy*, vol. 55, pp. 194–204, 2013.

[92] S. Baier, E. Fridman, S. Kliem, and U. Rohde, "Extension and application of the reactor dynamics code DYN3D for Block-type High Temperature Reactors," *Nucl Eng Des*, vol. 271, pp. 431–436, 2014.

[93] N. Martin and A. Hébert, "Adaptation of the B_1 leakage model to Monte Carlo criticality calculations," in *International Conference on Mathematics and Computational Methods Applied to Nuclear Science and Engineering (M&C 2011)*, (Rio de Janeiro, RJ, Brazil, May 8–12), 2011.

[94] E. M. Gelbard and R. Lell, "Monte Carlo Treatment of Fundamental-Mode Neutron Leakage in the Presence of Voids," *Nucl Sci Eng*, vol. 63, pp. 9–23, 1977.

[95] T. Yamamoto, "Monte Carlo algorithm for buckling search and neutron leakage-corrected calculations," *Ann Nucl Energy*, vol. 47, pp. 14–20, 2012.

[96] S. Yun and N. Z. Cho, "Monte Carlo Depletion Under Leakage-Corrected Critical Spectrum via Albedo Search," *Nucl Eng Technol*, vol. 42, no. 3, pp. 271–278, 2010.

[97] F. Rahnema and E. M. Nichita, "Leakage corrected spatial (assembly) homogenization technique," *Ann Nucl Energy*, vol. 24, no. 6, pp. 477–488, 1997.

[98] M. Tohjoh, M. Watanabe, and A. Yamamoto, "Application of continuous-energy Monte Carlo code as cross-section generator of BWR core calculations," *Ann Nucl Energy*, vol. 32, pp. 857–875, 2005.

[99] G. Ilas and F. Rahnema, "A Monte Carlo based nodal diffusion model for criticality analysis of spent fuel storage lattices," *Ann Nucl Energy*, vol. 30, pp. 1089–1108, 2003.

[100] E. L. Redmond II, *Multigroup Cross Section Generation via Monte Carlo Methods*. PhD thesis, Massachusetts Institute of Technology, 1997.

[101] J. F. Briesmeister, ed., "MCNP - A General Monte Carlo Code for Neutrons, Photons, and Electrons Transport, Version 4B," Tech. Rep. LA-12625-M, Los Alamos National Laboratory, 1997.

[102] E. Fridman, J. Leppänen, and C. Wemple, "Comparison of Serpent and HELIOS-2 as applied for the PWR few-group cross section generation," in *International Conference on Mathematics and Computational Methods Applied to Nuclear Science and Engineering (M&C 2013)*, (Sun Valley, Idaho, USA, May 5–9), 2013.

[103] T. Takeda, K. Kurihara, and M. Yamamoto, "Estimation of Anisotropic Effect of Diffusion Coefficient in a Fast Critical Assembly," *J Nucl Sci Technol*, vol. 11, no. 10, pp. 422–433, 1974.

[104] M. S. Milgram, "Estimation of Axial Diffusion Processes by Analog Monte Carlo: Theory, Tests and Examples," *Ann Nucl Energy*, vol. 24, no. 9, pp. 671–704, 1997.

[105] E. D. Cashwell and R. G. Schrandt, "Flux at a Point in MCNP," Tech. Rep. LA-UR-80-1167, Los Alamos National Laboratory, 1980.

[106] F. E. Harris, "Tables of the Exponential Integral Ei(x)," *Math Comput*, vol. 11, pp. 9–16, January 1957.

[107] C. J. Gho, *Homogénéisation du coefficient de diffusion: influence de la modélisation et du laplacien pour les réacteurs rapides de puissance et les maquettes expérimentales*. PhD thesis, Université Scientifique et Médicale de Grenoble, 1984.

[108] A. Khairallah and J. Recolin, "Calculation of the resonance self-shielding in complex cells by the method of sub-groups," in *Proceedings of a seminar on numerical reactor calculations*, IAEA-SM-154/37, pp. 305–317, 1972.

[109] W. F. G. van Rooijen, T. Hazama, and T. Takeda, "Monte Carlo Based Diffusion Coefficients for LMFBR Analysis," in *Joint International Conference on Supercomputing in Nuclear Applications and Monte Carlo 2010 (SNA+MC 2010)*, 2010.

[110] Y. Nagaya, K. Okumura, T. Mori, and M. Nakagawa, "MVP/GMVP II: General Purpose Monte Carlo Codes for Neutron and Photon Transport Calculations based on Continuous Energy and Multigroup Methods," Tech. Rep. JAERI-1348, Japan Atomic Energy Research Institute (JAERI), 2005.

[111] W. F. G. van Rooijen and G. Chiba, "Diffusion coefficients for LMFBR cells calculated with MOC and Monte Carlo methods," *Ann Nucl Energy*, vol. 38, pp. 133–144, 2011.

[112] E.M. Gelbard and R. Pego, "Monte Carlo computation of directional diffusion coefficients," Tech. Rep. FRA-TM-117, Argonne National Laboratory, 1979.

[113] R. C. Gast, "Procedure for obtaining neutron-diffusion coefficients from neutron-transport Monte Carlo calculations," Tech. Rep. WAPD-TM–1446, Bettis Atomic Power Laboratory, 1981.

[114] T. Yamamoto, "Monte Carlo method with complex weights for neutron leakage-corrected calculations and anisotropic diffusion coefficient generations," *Ann Nucl Energy*, vol. 50, pp. 141–149, 2012.

[115] E. Fridman and L. Leppänen, "Revised methods for few-group cross sections generation in the Serpent Monte Carlo code," in *ANS Reactor Physics Topical Meeting (PHYSOR 2012)*, (Knoxville, Tennessee, USA, April 15–20), 2012.

[116] E. Fridman, S. Duerigen, Y. Bilodid, D. Kotlyar, and E. Shwageraus, "Axial discontinuity factors for the nodal diffusion analysis of high conversion BWR cores," *Ann Nucl Energy*, vol. 62, pp. 129–136, 2013.

[117] A. Hall, Y. Xu, A. Ward, T. Downar, K. Shirvan, and M. Kazimi, "Advanced Neutronics Methods for Analysis of the RBWR-AC," in *Transactions of the American Nuclear Society*, vol. 108, pp. 771–774, 2013.

[118] N. Z. Cho, S. Yun, and J. Lee, "2-D Extension of the Global-Local Iteration Method with Homogenization by Monte Carlo Based on Non-Zero Leakage Spectra," in *Transactions of the Korean Nuclear Society Autumn Meeting*, October 2009.

[119] M. R. Zika and T. J. Downar, "Numerical Divergence Effects of Equivalence Theory in the Nodal Expansion Method," *Nucl Sci Eng*, vol. 115, no. 3, pp. 219–232, 1993.

[120] A. Yamamoto, "Convergence Improvement of Response Matrix Method with Large Discontinuity Factors," *Nucl Sci Eng*, vol. 145, pp. 291–298, 2003.

[121] D. Blanchet, L. Buiron, N. Stauff, T. K. Kim, and T. Taiwo, "AEN - WPRS Sodium Fast Reactor Core Definitions," Tech. Rep. version 1.2 - September 19^{th}, CEA and Argonne National Laboratory, 2011.

[122] R. E. MacFarlane, D. W. Muir, R. M. Boicourt, and A. C. Kahler, "The NJOY Nuclear Data Processing System, Version 2012," Tech. Rep. LA-UR-12-27079, Los Alamos National Laboratory, 2013.

[123] J. J. Herrero, N. García-Herranz, D. Cuervo, and C. Ahnert, "Neighborhood-corrected interface discontinuity factors for multi-group pin-by-pin diffusion calculations for LWR," *Ann Nucl Energy*, vol. 46, pp. 106–115, 2012.

[124] M. M. Bretscher, "Computing control rod worths in thermal research reactors," Tech. Rep. ANL/RERTR/TM-29, Argonne National Laboratory, February 1977.

[125] M. M. Bretscher, J. R. Deen, N. A. Hanan, J. E. Matos, S. C. Mo, R. B. Pond, A. Travelli, and W. L. Woodruff, "Relative performance properties of the ORNL Advanced Neutron Source Reactor with reduced enrichment fuels," Tech. Rep. ANL/TD/CP–85125, Argonne National Laboratory, September 1994.

[126] R. Kyrki-Rajamäki, *Three-dimensional reactor dynamics code for VVER type nuclear reactors*. PhD thesis, VTT Technical Research Centre of Finland, 1995.

[127] J. Loberg, M. Österlund, K.-H. Bejmer, J. Blomgren, and J. Kierkegaard, "Homogenization of Cross Sections and Computation of Discontinuity Factors for a Real 3D BWR Bottom Reflector for Comparison with Lattice and Nodal Codes," *Nucl Technol*, vol. 177, no. 1, pp. 1–7, 2012.

[128] K. Shirakata and T. Iijima, "Measurement of Anisotropy of Diffusion Coefficient in Plate Cell," *J Nucl Sci Technol*, vol. 14, no. 6, pp. 462–464, 1977.

[129] H. Gerwin and W. Scherer, "Treatment of the Upper Cavity in a Pebble-Bed High-Temperature Gas-Cooled Reactor by Diffusion Theory," *Nucl Sci Eng*, vol. 97, pp. 9–19, 1987.

[130] J. M. Pounders, F. Rahnema, D. Serghiuta, and J. Tholammakkil, "A 3D stylized half-core CANDU benchmark problem," *Ann Nucl Energy*, vol. 38, pp. 876–896, 2011.

[131] International Atomic Energy Agency (IAEA), "In-core fuel management benchmarks for PHWRs," Tech. Rep. IAEA-TECDOC-887, June 1996.

[132] J. M. Pounders, F. Rahnema, and D. Serghiuta, "Analysis of a multigroup stylized CANDU half-core benchmark," *Ann Nucl Energy*, vol. 38, pp. 2024–2078, 2011.

[133] W. Shen, "On the better performance of the coarse-mesh finite-difference method for CANDU-type reactors," *Ann Nucl Energy*, vol. 46, pp. 169–178, 2012.

[134] J. C. Gauthier, J. C. Cabrillat, G. Palmiotti, M. Salvatores, M. Giese, M. Carta, and J. P. West, "Measurement and Predictions of Control Rod Worth," *Nucl Sci Eng*, vol. 106, pp. 18–29, 1990.

Errata

Publication I

This article incorrectly references the work by Yamamoto:

- T. Yamamoto, "Monte Carlo algorithm for buckling search and neutron leakage-corrected calculations," *Ann Nucl Energy*, **47**, 14–20 (2012)

Instead, the correct reference should be:

- T. Yamamoto, "Monte Carlo method with complex weights for neutron leakage-corrected calculations and anisotropic diffusion coefficient generations," *Ann Nucl Energy*, **50**, 141–149 (2012)

Nuclear fission reactors are complex systems that involve several physical phenomena. The safe and sustainable operation of present-day reactors requires powerful numerical methods. Moreover, innovative reactor concepts pose an additional burden on the computational techniques available nowadays.

This thesis explores the performance of preexisting and novel numerical formalisms for the solution of the steady-state neutron transport problem by combined Monte Carlo and diffusion theory methods with a view to improving the accuracy of the solution whilst keeping computational costs at reasonable levels.

A new directional diffusion coefficient method exhibited very good performance in a sodium-cooled reactor environment. A novel neutron leakage model at assembly level provided valuable information about the space-energy coupling of the scalar neutron flux.

Aalto-DD 60/2016

ISBN 978-952-60-6735-3 (printed)
ISBN 978-952-60-6736-0 (pdf)
ISSN-L 1799-4934
ISSN 1799-4934 (printed)
ISSN 1799-4942 (pdf)

Aalto University
School of Science
Department of Applied Physics
www.aalto.fi